

# NOTE TO USERS

This reproduction is the best copy available.

**UMI**<sup>®</sup>



**University of Alberta**

**SKELETAL MUSCLE REPAIR AFTER DENERVATION INJURY**

**by**

**Yang Shu**



A thesis submitted to the Faculty of Graduate Studies and Research in partial fulfillment of the requirements for the degree of Master of Science

Faculty of Physical Education and Recreation

Edmonton, Alberta

Fall, 2005



Library and  
Archives Canada

Bibliothèque et  
Archives Canada

Published Heritage  
Branch

Direction du  
Patrimoine de l'édition

395 Wellington Street  
Ottawa ON K1A 0N4  
Canada

395, rue Wellington  
Ottawa ON K1A 0N4  
Canada

*Your file* *Votre référence*  
*ISBN: 0-494-09287-4*  
*Our file* *Notre référence*  
*ISBN: 0-494-09287-4*

**NOTICE:**

The author has granted a non-exclusive license allowing Library and Archives Canada to reproduce, publish, archive, preserve, conserve, communicate to the public by telecommunication or on the Internet, loan, distribute and sell theses worldwide, for commercial or non-commercial purposes, in microform, paper, electronic and/or any other formats.

The author retains copyright ownership and moral rights in this thesis. Neither the thesis nor substantial extracts from it may be printed or otherwise reproduced without the author's permission.

**AVIS:**

L'auteur a accordé une licence non exclusive permettant à la Bibliothèque et Archives Canada de reproduire, publier, archiver, sauvegarder, conserver, transmettre au public par télécommunication ou par l'Internet, prêter, distribuer et vendre des thèses partout dans le monde, à des fins commerciales ou autres, sur support microforme, papier, électronique et/ou autres formats.

L'auteur conserve la propriété du droit d'auteur et des droits moraux qui protègent cette thèse. Ni la thèse ni des extraits substantiels de celle-ci ne doivent être imprimés ou autrement reproduits sans son autorisation.

---

In compliance with the Canadian Privacy Act some supporting forms may have been removed from this thesis.

Conformément à la loi canadienne sur la protection de la vie privée, quelques formulaires secondaires ont été enlevés de cette thèse.

While these forms may be included in the document page count, their removal does not represent any loss of content from the thesis.

Bien que ces formulaires aient inclus dans la pagination, il n'y aura aucun contenu manquant.

  
**Canada**

## ABSTRACT

A deficiency of muscle satellite cells seems to underlie some of the incomplete recovery of skeletal muscle structure and function after a period of prolonged denervation. However, the contribution of satellite cells to muscle recovery when innervation is re-established has not been fully explored. The purpose of this study was to investigate if limiting muscle satellite cells by  $\gamma$ -irradiation would impede the recovery of the rat atrophied *tibialis anterior* muscle after reinnervation. Twenty-four Sprague-Dawley rats were subjected to repeated crush injury of the *common peroneal* nerve to induce prolonged denervation of the *tibialis anterior* muscle (~70 days) followed by reinnervation. When reinnervation commenced, twelve of the rats were exposed to  $\gamma$ -irradiation focused on the *tibialis anterior* muscle, with the remainder of the animal shielded in 2.5 cm thick lead to block satellite cell activity for 12 weeks; the other twelve rats were allowed to recover normally. Similar recovery was observed in both groups, suggesting that proliferation of satellite cells during denervation produced enough progeny for subsequent regeneration when innervation was re-established. However, a limited satellite cell pool reflected by the decreased myonuclei and quiescent satellite cell numbers seems partially responsible for the poor recovery of skeletal muscle after prolonged denervation.

## **ACKNOWLEDGEMENTS**

I would like to take the opportunity to genuinely thank all my committee members Dr. Ted Putman (supervisor), Dr. Tessa Gordon, Dr. George Foxcroft and Dr. Walter Dixon for their knowledge, guidance and patience. In addition, a thank you to Dr. Gordon Bell who provided me with much support during my M.Sc.

I would also like to express my gratitude to numerous others who assisted me throughout the course of my study. Firstly, a special thank you to Neil Tyreman, Ian MacLean and Jean Pearcey for all their technical assistance as well as their encouragement. In addition, I would like to express my appreciation to other students who made my entire laboratory experience an enjoyable one. Namely, Karen Martins, Maria Gallo and Winnie Wong for their invaluable support when it was most required. I am also grateful to the Faculty of Physical Education & Recreation for their support over the duration of my degree. This work was funded by AHFMR and NSERC.

Finally, a big thank you to my family and my friends, Wenjun Zhang, Hui Zheng, Liushi Gan, Tianyi Liu, and Xiaoran Sun, who have been and will always be supportive throughout my various endeavours.

## TABLE OF CONTENTS

<b>CHAPTER I: INTRODUCTION.....</b>	<b>1</b>
<u>Introduction</u> .....	1
<u>Purpose</u> .....	2
<u>Significance of Study</u> .....	2
<u>Hypothesis</u> .....	2
<u>Delimitations</u> .....	3
<u>Limitations</u> .....	4
<b>CHAPTER II: LITERATURE REVIEW.....</b>	<b>5</b>
<u>Part 1: Satellite Cells</u> .....	5
<i>Definition and Identification</i> .....	5
<i>Distribution</i> .....	9
<i>Function in Muscles</i> .....	11
<i>Heterogeneity</i> .....	13
<i>Regulatory Factors</i> .....	13
<i>Proliferation Capacity</i> .....	16
<i>Aging</i> .....	17
<i>Effects of Low-Dose Ionizing Irradiation</i> .....	19
<u>Part 2: Peripheral Nerve Injury</u> .....	21
<i>Morphological and Functional Changes</i> .....	21
<i>Cell and Nuclear Death</i> .....	22
<i>Reinnervation Capacity of Muscle</i> .....	23
<i>Reinnervation Capacity of Motor Nerve</i> .....	24
<i>Satellite Cell Activation and Depletion</i> .....	25
<b>CHAPTER III: METHODS.....</b>	<b>28</b>
<u>Part 1: Experimental Model</u> .....	28
<i>Experimental Animals</i> .....	28
<i>Repeated Nerve Crush Injury</i> .....	28
<i>Gamma (<math>\gamma</math>)-Irradiation Treatment</i> .....	29
<i>Muscle Sample Preparation</i> .....	30
<u>Part 2: Analyses</u> .....	31
<i>Functional Measurements</i> .....	31
<i>Antibodies</i> .....	34
<i>Immunohistochemistry for Myosin Heavy Chain Isoforms, Desmin,     Vimentin and Dystrophin</i> .....	35
<i>Immunohistochemistry for Collagen IV with Laminin, PCNA,</i>	

<i>M-cadherin and Myogenin</i> .....	37
<i>Immunohistochemistry for NCAM</i> .....	37
<i>Harris' Haematoxylin with Eosin Stain</i> .....	38
<i>Morphometric Fibre Analyses</i> .....	38
<i>Electrophoretic Analysis of MHC Isoforms</i> .....	39
<i>Statistical Analysis</i> .....	40
<b>CHAPTER IV: RESULTS</b> .....	42
<u>Functional Measures</u> .....	42
<u>Reinnervation</u> .....	42
<u>Myonuclear Content and Satellite Cell Activity</u> .....	42
<u>Fibre Cross-Sectional Area</u> .....	43
<u>Fibre Type Transitions</u> .....	44
<b>CHAPTER V: DISCUSSION</b> .....	59
<u>Introduction</u> .....	59
<u>Muscle Reinnervation</u> .....	60
<u>Structural and Functional Recovery After Reinnervation</u> .....	61
<u>Muscle Fibre Type Transition</u> .....	64
<u>Satellite Cell Involvement</u> .....	65
<u>Future Research Directions</u> .....	67
<u>Conclusion</u> .....	68
<b>CHAPTER VI: LIST OF REFERENCE</b> .....	70



## LIST OF TABLES

Table 4-1:	Body mass, muscle mass, and crushed-to-control muscle mass ratio of rat <i>tibialis anterior</i> .	45
Table 4-2:	Muscle mean motor unit twitch force, motor unit number and crushed-to-control muscle twitch ratio of rat <i>tibialis anterior</i> .	46

## LIST OF FIGURES

Figure 2-1:	Summary of molecules regulating satellite cell activity.	15
Figure 3-1:	Summary of the experimental design.	30
Figure 3-2:	Schematic representation of whole muscle and motor unit twitch force recordings. (A) <i>Tibialis anterior</i> muscles were isolated by denervating all other hindlimb muscles and attached to a force transducer. Ventral roots L4-L5 were isolated and split for stimulation of single motor axons contributing to <i>tibialis anterior</i> muscle; (B) Twitch contraction of the whole muscle was elicited by maximal nerve stimulation; (C) ventral root filaments were teased so that stimulation elicited all-or-none increments of force in the <i>tibialis anterior</i> muscle.	32
Figure 4-1:	Isometric functional properties of <i>tibialis anterior</i> muscles: (A) twitch force; (B) time to peak force; (C) half force rise time; (D) half force fall time; (E) tetanus force; (F) SAG ratio.	47
Figure 4-2:	Changes in the isometric functional properties of the treated <i>tibialis anterior</i> muscles relative to their respective contralateral controls. The values of contralateral controls are 100%. Data are calculated from those displayed in Figure 4-1. (A) twitch force; (B) time to peak force; (C) half force rise time; (D) half force fall time; (E) tetanus force; (F) SAG ratio.	48
Figure 4-3:	Representative NCAM stains of <i>tibialis anterior</i> muscles: (A) contralateral control of muscle shown in C; (B) contralateral control of muscle shown in D; (C) nerve crushed <i>tibialis anterior</i> muscle; (D) irradiated & nerve crushed <i>tibialis anterior</i> muscle.	49
Figure 4-4:	Representative photomicrographs of (A) H&E, (B) myogenin, (C) M-cadherin and (D) PCNA staining.	50
Figure 4-5:	Positively stained myonuclei number per mm <sup>2</sup> (A) H&E, (B) myogenin, (C) M-cadherin and (D) PCNA.	51
Figure 4-6:	Positively stained myonuclei number per mm <sup>2</sup> corrected for fibre atrophy (A) H&E, (B) myogenin, (C) M-cadherin and (D) PCNA.	52

Figure 4-7:	Changes in the positively stained myonuclei number per mm <sup>2</sup> (corrected for fibre atrophy) of the treated <i>tibialis anterior</i> muscles relative to their respective contralateral control. The values of contralateral control are 100%. Data are calculated from those displayed in Figure 4-6. (A) H&E, (B) myogenin, (C) M-cadherin and (D) PCNA.	53
Figure 4-8:	Representative photomicrographs of MHC immunostaining from contralateral control (A, B, C, D) and nerve crushed (E, F, G, H) <i>tibialis anterior</i> muscles. Sections are stained with: BA-D5 (type I - A, E); SC-71 (type IIA - B, F); BF-35 (invert stain of type IID(X) - C, G) and BF-F3 (type IIB - D, H).	54
Figure 4-9:	Muscle fibre cross-sectional area for each fibre type and the average for all fibres (hybrid fibres are counted as both types they express)	55
Figure 4-10:	Muscle fibre cross-sectional area for each fibre type (hybrid fibres are counted separately).	56
Figure 4-11:	Changes in the muscle fibre cross-sectional areas of the treated <i>tibialis anterior</i> muscles relative to their respective contralateral control. The values of contralateral are 100%. Data are calculated from those displayed in Figure 4-9.	57
Figure 4-12:	Changes in the muscle fibre cross-sectional area for each fibre type (hybrid are counted separately) of the treated <i>tibialis anterior</i> muscles relative to their respective contralateral controls. The values of contralateral controls are 100%. Data are calculated from those displayed in Figure 4-10.	58
Figure 4-13:	Fibre type percentage analyzed by immunohistochemistry (hybrid fibres are counted as both types they express).	59
Figure 4-14:	Fibre type percentage analyzed by immunohistochemistry (hybrid fibres are counted separately).	60
Figure 4-15:	Changes in the fibre type percentage of the treated <i>tibialis anterior</i> muscles relative to their respective contralateral controls. The values of contralateral controls are 100%. Data are calculated from those displayed in Figure 4-13.	61

Figure 4-16:	Changes in the fibre type percentage (hybrid fibres are counted separately) of the treated <i>tibialis anterior</i> muscles relative to their respective contralateral controls. The values of contralateral controls are 100%. Data are calculated from those displayed in Figure 4-14.	62
Figure 4-17:	Representative MHC separation via SDS-PAGE.	63
Figure 4-18:	MHC content analyzed by SDS-PAGE.	64
Figure 4-19:	Changes in the MHC content of the treated <i>tibialis anterior</i> muscles relative to their respective contralateral controls. The values of contralateral controls are 100%. Data are calculated from those displayed in Figure 4-18.	65

## LIST OF ABBREVIATIONS

ABC = avidin-biotin-peroxidase complex  
BSA = bovine serum albumin  
CSA = cross-sectional area  
DAB = 3'diaminobenzidine tetrahydrochloride  
DNA = deoxyribonucleic acid  
DTT = dithiothreitol  
EDTA = ethylenediaminetetraacetic acid  
EGTA = ethylenebis(oxyethylenenitrilo)tetraacetic acid  
FGF = fibroblast growth factor  
FITC = fluorescein isothiocyanate  
g = gram  
H<sub>2</sub>O<sub>2</sub> = hydrogen peroxide  
HCl = hydrochloric acid  
HGF = hepatocyte growth factor  
IGF = insulin-like growth factor  
IgG = immunoglobulin G  
IgM = immunoglobulin M  
IL = interleukin  
KOH = potassium hydroxide  
LIF = leukemia inhibitory factor  
MGF = mechano growth factor  
MHC = myosin heavy chain  
mM = millimolar  
mN = millinewton  
MRF = myogenic regulatory factor  
mRNA = messenger RNA  
ms = millisecond  
µg = microgram  
µl = micro litre  
NADH = nicotinamide adenine dinucleotide (reduced form)  
NCAM = neural-cell adhesion molecule  
PAGE = polyacrylamide gel electrophoresis  
PBS = phosphate-buffered saline  
RNA = ribonucleic acid  
RPM = revolutions per minute  
RT-PCR = reverse transcriptase-polymerase chain reaction  
SDS-PAGE = sodium dodecyl sulfate polyacrylamide gel electrophoresis  
TBS = Tris-buffered saline  
TGF = transforming growth factor  
V = volts

## CHAPTER I: INTRODUCTION

### Introduction

Skeletal muscle can be seen as an extension of the peripheral nervous system, because its differentiation, structural maintenance, and function are directly regulated by its motor nerve supply (Viguie *et al.*, 1997). A denervated muscle will gradually atrophy over a period of time and lose its mass and contractile function, and the muscle fibres will undergo a series of changes in structure, biochemistry, and physiology (Viguie *et al.*, 1997; Stonnington & Engel, 1973; Sunderland & Ray, 1950).

Despite the impressive regenerative potential of peripheral nerves, recovery of skeletal muscle structure and function after a period of prolonged denervation is generally poor (Fu & Gordon, 1995a). The principle cause has been suggested to be the failure of some axons to reach denervated muscle fibres due to the progressive degeneration of the basement membrane, which serves as a protective nerve sheath (Fu & Gordon, 1995a). It has been further suggested that incomplete recovery of previously denervated muscle fibres was also related to intrinsic factors associated with muscle fibres. In this regard, one of the possible factors concerns a small group of cells that reside in adult skeletal muscle and that are referred to as satellite cells. Depletion of this endogenous population of muscle stem cells committed to a myogenic lineage would seem to underlie some of the incomplete recovery. Although satellite cells represent only a minor portion (2-7%) of total muscle nuclei associated with adult fibres (Schultz

& McCormick, 1994), they possess a very large capacity for self-renewal and are the source of new postmitotic muscle nuclei during fibre growth and of new fibres during muscle regeneration (Schultz, 1989; Hawke & Garry, 2001; Schultz & McCormick, 1994).

### **Purpose**

The purpose of this study was to investigate 1) the extent to which reinnervated skeletal muscle fibres of the *tibialis anterior* recover their structural and functional properties after prolonged denervation, and 2) if limiting the contribution of the muscle satellite cell population impedes the recovery process.

### **Significance of Study**

The results of this study have enhanced our understanding of the functional role of muscle satellite cells in the recovery of skeletal muscle fibres from neuromuscular trauma. Specifically, this study sheds light on whether or not recovery from nerve trauma is impeded by attenuating the contribution of satellite cells. Therefore, it allows us to appreciate if the satellite cell population is a limiting factor for muscle recovery from denervation atrophy and to evaluate the rationale of using cell transplantation to enhance the recovery.

### **Hypothesis**

The effects of prolonged denervation on muscle fibre structure and function have been demonstrated to be fibre atrophy and poor recovery even after the muscle is reinnervated. This may be due to a limitation in the muscle satellite

cell population. It was hypothesized that denervated left *tibialis anterior* muscles would display decreased muscle fibre cross-sectional areas, and decreased muscle force with greater satellite cell activity during recovery. However, when  $\gamma$ -irradiation is super-imposed on repeated nerve crush injuries, we hypothesized that satellite cell activity to be reduced.

### **Delimitations**

In order to restrict our analysis to the intrinsic muscle factors, we employed a regime of repeated crushes (Bridge *et al.*, 1994) applied to the *common peroneal* nerve, rather than complete nerve ligation employed by Fu and Gordon (1995). This allowed us to retain the integrity of the basement membrane, associated Schwann cells, and the substrate and trophic support afforded to regenerating axons by these structures. This modification of the studies by Fu and Gordon (1995) eliminated potential degeneration of the basement membrane which otherwise could influence recovery following reinnervation. In addition parallel experiments were completed in which the satellite cell population of the *tibialis anterior* muscle was sterilized by very focused and repeated exposure to 30-Gy of ionizing radiation every 4-weeks during the recovery period from prolonged denervation (Phelan & Gonyea, 1997; Wakeford *et al.*, 1991). Energy from  $\gamma$ -irradiation causes DNA disruption in the pre-mitotic satellite cells and thus prevents mitosis (Gillies, 1987). However, since skeletal muscle fibres are post-mitotic, gene expression in myonuclei remains unaffected (Rosenblatt & Parry, 1992; Rosenblatt & Parry, 1993; Rosenblatt *et al.*, 1994; Phelan & Gonyea, 1997).



## **Limitations**

According to Phelan and colleague's study (1997), a single dose of 30-Gy  $\gamma$ -irradiation should block satellite cell activation for up to 4 weeks. However, other studies suggested that a single dose of 25-Gy  $\gamma$ -irradiation could only sustain its effect for 7 days, as satellite cells possess the ability for DNA repair and mitotic recovery from a single dose of ionizing radiation (Mozdziak *et al.*, 1996; Gillies, 1987). This limitation was addressed by administering a 30-Gy dose of  $\gamma$ -irradiation every 4 weeks in order to maintain a sterilized satellite cell population. The time point chosen in the study was based on the nerve regeneration properties from a pilot study. The  $\gamma$ -irradiation was first conducted on day 70 because after the last nerve crush, 28 days were necessary for the nerve to grow back to the muscle. Although during this time period satellite cells could have been proliferating, we had to allow this because if  $\gamma$ -irradiation was conducted before reinnervation, the results would not be comparable between the two groups since nerve regeneration might be affected by the  $\gamma$ -irradiation, as Love (1983) has shown that a 20-Gy irradiation reduced endoneurial cellular proliferation. Furthermore, a 4-week interval between  $\gamma$ -irradiation treatments was chosen because, although a more frequent application of  $\gamma$ -irradiation would ensure a complete sterilization of satellite cells, it could also put too much stress on the rats and result in a high mortality rate.

## **CHAPTER II: LITERATURE REVIEW**

### **Part 1: Satellite Cells**

#### ***Definition and Identification***

Mauro (1961) described a group of cells closely associated with the periphery of the frog myofibre and termed them satellite cells based on their location. Satellite cells are physically distinct from the adult myofibre as they reside within indentations between the sarcolemma and the basal lamina (Hawke & Garry, 2001). These cells are a feature of postnatal and adult muscle, and continue to be defined according to morphological criteria. No other cell type is located in this position (Schultz & McCormick, 1994). In summary, satellite cells are undifferentiated mononuclear, quiescent, muscle precursor cells located between the basal lamina and the sarcolemma in postnatal and adult muscle fibres (Putman *et al.*, 1999; Schultz & McCormick, 1994).

Based on its definition, satellite cells can be identified as mononuclear cells at the periphery of the mature, multinucleated myofibres. Although satellite cells have morphological features that are different from myonuclei. Unfortunately, as satellite cells lack any distinguishing morphological characteristics that allow light microscopic quantitative or qualitative studies, they can only be positively recognized at the electron microscope level (Schultz & McCormick, 1994).

At the light microscope level, however, some methods have been developed to morphologically identify satellite cells. By staining the nuclei, plasmalemma and basal lamina of a muscle fibre using triple staining with haematoxylin, dystrophin, and laminin, satellite cells can be recognized as nuclei located between these membranes (Zhang & McLennan, 1994; Putman *et al.*, 1999).

In the past few years a variety of satellite cell-specific markers have been identified that have allowed researchers to study satellite cells at the light microscope level. Markers have been identified that are only expressed in quiescent, activated or proliferating satellite cells, respectively, or are expressed more broadly throughout the cell cycle (Hawke & Garry, 2001). The family of myogenic regulatory factors (MRFs), a group of helix-loop-helix transcription factors, is expressed in activated satellite cells, including myogenin, myoD, myf5 and MRF4. Although none of these MRFs are detectable in quiescent satellite cells, most of activated satellite cells begin to express either MyoD or myf5 first, and then most cells express both myf-5 and MyoD simultaneously (Cornelison & Wold, 1997; Sabourin & Rudnicki, 2000). MRF4 is detectable later in cells expressing both MyoD and myf5. In the last phase myogenin is expressed during the time associated with differentiation leading to fusion with muscle fibres. Many cells may ultimately express all four MRFs simultaneously (Yablonka-Reuveni & Rivera, 1994; Smith *et al.*, 1994). As a result, the staining of nuclei for myogenin is used to detect satellite cell progeny that had become committed to, or are in the later stages of, terminal differentiation (Putman *et al.*, 2000; Putman *et al.*, 1999; Yablonka-Reuveni & Rivera, 1994).

Muscle-cadherin (M-cadherin), a calcium-dependent transmembrane glycoprotein that is expressed at the boundary between the satellite cell and the adjacent fibre, is recognized as a unique marker for quiescent satellite cells (Irintchev *et al.*, 1994; Kuschel *et al.*, 1999). When muscle regeneration is at its early stages, M-cadherin expression is transiently up-regulated, which is a result of an up-regulated satellite cell population (Kaufmann *et al.*, 1999; Irintchev *et al.*, 1994). After these myoblasts fuse into myotubes, this tide of expression fades away and eventually there is no detectable M-cadherin in the mature myotubes (Kaufmann *et al.*, 1999; Irintchev *et al.*, 1994). Although a high proportion of satellite cells in intact muscles was claimed to be positive for anti-M-cadherin antibodies (Irintchev *et al.*, 1994; Irintchev *et al.*, 1997), a study based on *in vitro* experiments showed that M-cadherin is only expressed in a subpopulation of the quiescent cell pool in intact muscle (Cornelison & Wold, 1997). Nevertheless, it is believed that M-cadherin is crucial for myogenic morphogenesis and functions as a molecular link between the satellite cell and the adjacent muscle fibre (Kaufmann *et al.*, 1999). Besides M-cadherin, other cell adhesion molecules may also be potential markers for quiescent satellite cells, including neural cell adhesion molecule (NCAM) and vascular adhesion molecule-1 (VCAM-1) (Hawke & Garry, 2001). NCAM is expressed in both myofibres and satellite cells, but VCAM-1 is only present in satellite cells in adult muscle (Covault & Sanes, 1986; Jesse *et al.*, 1998). In addition, VCAM-1 was shown to mediate satellite cell interaction with leukocytes following injury (Jesse *et al.*, 1998).

Techniques for identifying proliferating satellite cells include [<sup>3</sup>H]thymidine (Moss & Leblond, 1971), bromodeoxyuridine (BrdU) (Schultz, 1996) labeling, and proliferating cell nuclear antigen (PCNA) expression. Cells synthesizing DNA in preparation for mitosis can be identified by pulse or continuous labeling with radiolabelled isotopes, such as [<sup>3</sup>H]thymidine, or with the non-radioactive thymidine analogue 5'-bromo-deoxyuridine (BrdU) (Lawson-Smith & McGeachie, 1998). The former is detected by prolonged exposure to x-ray film, while the later is detected using a monoclonal anti-BrdU antibody and standard immunohistochemical procedures. PCNA is an acidic nonhistone auxiliary protein of DNA polymerase and is only expressed during DNA synthesis (Bravo *et al.*, 1987). Thus PCNA immuno-reactivity can be used to identify cells in the S-phase of the cell cycle, and to quantify the fraction of satellite cells that are dividing (Schultz, 1996; Johnson & Allen, 1993; Moss & Leblond, 1971).

Desmin is a protein found in the intermediate filaments of the cytoskeleton of muscle cells (Lazarides & Hubbard, 1976) and its expression can help identify muscle precursor cells at a very early stage of the myogenic cycle after muscle injury (Roberts *et al.*, 1997). It has been suggested that desmin labeling can be used to identify muscle precursor cells very soon after injury (Lawson-Smith & McGeachie, 1998). Another potential marker of quiescent satellite cells is called c-Met, the receptor for hepatocyte growth factor (HGF) (Cornelison & Wold, 1997). It has been reported the c-Met-deficient embryos failed to form limb skeletal muscle due to a lack of myogenic precursor cells (Maina *et al.*, 1996).

## ***Distribution***

Satellite cells are found in all vertebrate skeletal muscles, although the population is not evenly distributed across species, age, muscle location, or fibre type. At the present time, the most widely used method to describe satellite cell number is by expressing them as a proportion of the total myonuclear content (myonuclei plus satellite cells).

It is well-established that the densities of satellite cell populations differ within oxidative and glycolytic muscles, and there is always a higher number of satellite cells associated with predominantly oxidative muscles (Schultz, 1984). This could be explained by the idea that the innervating nerve determines the proportion of satellite cell nuclei in a muscle. For example, Schultz (1984) found that following cross-transplantation, the proportion of satellite cell in the fast-twitch *extensor digitorum longus* muscle regenerated in the slow-twitch *soleus* muscle bed was indistinguishable from the proportion in the control *soleus*. When the *soleus* muscle regenerated in the *extensor digitorum longus* bed, the graft *soleus* had a satellite cell proportion similar to the *extensor digitorum longus*. These results support the idea that the innervating nerve determines the proportion of satellite cells in a muscle.

Muscle fibre myonuclei have a similar pattern of distribution as satellite cells. The higher density of myonuclei in predominantly oxidative muscles than in predominantly glycolytic muscles, might be related to smaller “nuclear domains” or domains of fibre cytoplasm surrounded, and controlled, by each

individual myonucleus (Schultz & Darr, 1990). Smaller “nuclear domains” are presumably a requirement in oxidative muscles since there is a higher biosynthetic activity in these fibres. As a result, there is a higher demand for the production of myonuclei in predominantly oxidative muscles, which could also explain the higher density of satellite cells seen in these muscles. In summary, the size of the satellite cell population in a muscle appears to be governed by innervation or function of the muscle.

The distribution of satellite cells on fibres within a muscle is similar to that observed in entire muscles. In the same muscle, oxidative fibres demonstrate five-to-six fold greater satellite cell content (Gibson & Schultz, 1982). A possible reason for the difference could be the innervation or recruitment pattern of individual fibre types; since the oxidative fibres are recruited more frequently, there is a higher satellite cell reservoir associated with them (Schultz & McCormick, 1994).

On the same fibre, satellite cells are more concentrated in the proximity of motoneuron junctions, while in the extra-junctional regions, they are distributed evenly along the length of the fibres (Snow, 1981; Gibson & Schultz, 1982). Although the exact functions of junction-associated satellite cells need further investigation, Schultz & Darr (1990) suggested it could be related to the preservation of the junction, or synthesis of molecules important for its structure or function.

### ***Function In Muscles***

Although satellite cells are quiescent in normal adult muscles, they can become active and proliferate in response to a number of stimuli including muscle damage, denervation, stretching, overload, and adaptation to exercise (Putman *et al.*, 1999; Schultz & McCormick, 1994). During normal muscle growth, the major function of satellite cells seems to be to maintain a constant myonuclear-to-myoplasmic volume ratio by increasing myonuclei in myofibres (Darr & Schultz, 1987; Rosenblatt *et al.*, 1994; Schultz & Darr, 1990). Following a mitotic division, one or both daughter cells fuse with the adjacent myofibre, thereby contributing a new nucleus to the fibre syncytium (Schultz, 1989).

In adult and growing muscle, satellite cells also function as a cell source for skeletal muscle repair and regeneration after injury (McCormick & Thomas, 1992; Schultz & McCormick, 1994) by proliferating, terminally differentiating, and either fusing to existing muscle fibres or fusing to each other and forming new myofibres (Hawke & Garry, 2001). Elevated satellite cell mitotic activity can be a sensitive indicator of muscle damage 3 to 5 days after injury, especially when the damage is minimal and difficult to detect by morphological means (Schultz, 1989). Therefore, proliferation of satellite cells in the muscle is an important component of a regeneration response (Schultz, 1989).

Another muscle adaptation that involves satellite cell activation is the response to exercise. When the exercise induces any degree of myofibre damage, an increased proliferative behavior of satellite cells will arise. This



response is so sensitive that after a single bout of prolonged eccentric treadmill running, satellite cells were activated not only on fibres exhibiting overt necrosis, but also on those with lesions not discernible with light microscopy (Darr & Schultz, 1987). Load-induced hypertrophy also requires the participation of satellite cells. Resistance training induces muscle hypertrophy through a process of satellite cell activation, proliferation, chemotaxis, and fusion to existing myofibres (Rosenblatt *et al.*, 1994). This is also a result of the myofibre microdamage caused by the load. However, when satellite cell activity was blocked by  $\gamma$ -irradiation, compensatory hypertrophy induced by ablation of a synergist could not be seen (Rosenblatt & Parry, 1992; Rosenblatt *et al.*, 1994; Rosenblatt & Parry, 1993), providing evidence that the contribution of satellite cells to the compensatory myonuclei production.

Satellite cells may also play a role in fibre transformation. It is well known that under cross-innervation, there is a rapid transformation of fibre types: former fast fibres demonstrate many slow fibre characteristics and slow fibres shift toward fast fibres (Romanul & Van der Meulen, 1967). Based on this evidence, a model of low-frequency-stimulation has been used to elicit a fast-to-slow fibre-type transformation. It is postulated that the increase in muscle nuclei of the fast fibres might be a prerequisite for fast-to-slow fibre type transitions (Putman *et al.*, 2000), and that this increase is due to satellite cell proliferation and fusion (Putman *et al.*, 2000, 2001).

### ***Heterogeneity***

The view that satellite cells comprise at least two, and likely more, distinct sub-populations is becoming more accepted (Schultz & McCormick, 1994; Schultz, 1996; Baroffio *et al.*, 1996; Yoshida *et al.*, 1998; Hawke & Garry, 2001). Schultz (1996) found two distinct satellite cell compartments in growing skeletal muscle. About 80% of satellite cells divide quickly (32-hour cell cycle) and are the sole donors of post-mitotic skeletal muscle myonuclei, and the other 20% divide more slowly and may represent a reserve compartment that supplies the quickly dividing compartment. Interestingly, this minor subpopulation which divides slowly *in vitro* was reported to be activated and began rapid and extensive proliferation upon grafting into regenerating host muscle (Beauchamp *et al.*, 1999), whereas the majority of the satellite cells undergo rapid necrotic death. The apparent functional heterogeneity of the satellite cell population suggests that further study of the precise origins and lineage of satellite cells is required.

### ***Regulatory Factors***

The activation of satellite cells into the mitotic compartment and their progression to the differentiative compartment are processes which are tightly regulated by myogenic regulatory factors of the MyoD family and the cyclin-dependent kinases and their inhibitors (Bornemann *et al.*, 1999). These factors are in turn regulated by innervation and growth factors, such as insulin-like growth factors (IGFs) including IGF-I and IGF-II, hepatocyte growth factor (HGF), and fibroblast growth factor-6 (FGF-6), as summarized in figure 2-1.

IGF-I and IGF-II were found to increase satellite cell proliferation and differentiation *in vitro* (Haugk *et al.*, 1995). It was reported that following muscle damage, mechano growth factor (MGF), one of IGF-I splice variants, is expressed rapidly before MRFs expression, indicating it may be responsible for satellite cell activation (Hill & Goldspink, 2003). In *in vivo* studies, increased satellite cell differentiation and proliferation are also observed in transgenic mice that over-express IGF-I, as shown by increased expression of Cyclin D1, MyoD, and myogenin (Rabinovsky *et al.*, 2003). IGF-I administration into older animals also dramatically increased the proliferative potential of satellite cells and the mass of the injured muscle (Chakravarthy *et al.*, 2000). These studies demonstrated that local expression of IGF could improve the repair capacity of injured muscle.

Hepatocyte growth factor (HGF) is a potent mitogen for satellite cells and has been shown to be important in the migration of the myogenic precursor cells from the somite to the developing limb (Andermarcher *et al.*, 1996; Bladt *et al.*, 1995). Injection of HGF into muscle at the time of injury increases myoblast number by activating satellite cells to proliferate. However, down-regulation of HGF is necessary to allow terminal differentiation and fusion of myoblasts to form multinucleated myofibres, since it also acts directly on primary muscle cells to block differentiation and inhibit regeneration (Anastasi *et al.*, 1997; Miller *et al.*, 2000).

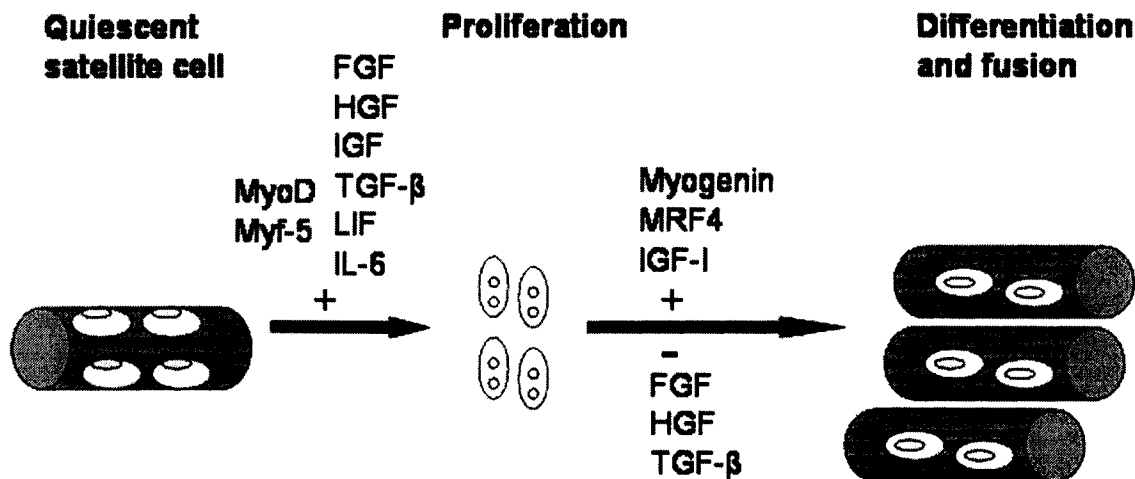


**Figure 2-1.** Summary of molecules regulating satellite cell activity.

Fibroblast growth factor-6 (FGF-6), one of nine isoforms of FGF, is expressed only in skeletal muscle and has been proposed to regulate the proliferation of satellite cells (Floss *et al.*, 1997). Like HGF, although the FGF family can activate satellite cells into proliferation, they also attenuate satellite cell differentiation to myofibres (Hawke & Garry, 2001). In addition, transforming growth factor- $\beta$  (TGF- $\beta$ ) has been reported to attenuate the activation of MyoD family members, thus inhibiting satellite cell proliferation and differentiation (Hawke & Garry, 2001).

Other factors such as interleukin-6 (IL-6) and leukemia inhibitory factor (LIF) are also involved in regulating satellite cell activity. It has been suggested that LIF acts as a stimulus for satellite cells while IL-6 promotes the degradation of necrotic tissue, thus playing an integral role in skeletal muscle regeneration (Hawke & Garry, 2001).

### ***Proliferation Capacity***

Satellite cells may have a limited capacity for replication. In culture, isolated satellite cells show a decline in proliferation rate over time, and eventually these cells will cease to divide when they reach a stage called proliferative senescence (Renault *et al.*, 2000). The major and most commonly observed determinant that alters the ability of satellite cells to produce progeny appears to be the previous proliferative history of the cells as determined by growth, disease, or injury. In these cases, if the satellite cell population has been forced into a mode of nearly continuous proliferation over an extended duration, it eventually leads to a significant reduction in the mitotic reserve of the cells (Schultz & McCormick, 1994). An insufficient satellite cell population has been reported to be related to the poor restorative capacity of atrophic muscles (Viguie *et al.*, 1997). Some diseases such as Duchenne Muscular Dystrophy (DMD), which results in continuous degeneration-regeneration cycles, are thought to ultimately exhaust the satellite cell pool (Hawke & Garry, 2001). Long-term denervation can also result in an initial rise and subsequent fall in satellite cell number (Viguie *et al.*, 1997). One possible reason for this change is that satellite cells become incorporated into atrophying or newly forming muscle fibres at a greater rate than their reproduction, thus the population is eventually depleted.

The satellite cell population exhibits a number of interesting differences as a function of age or in individual muscles. In both cases, as age progresses the proliferative capacity of satellite cells decreases (Hawke & Garry, 2001). In aged rats, Chakravarthy *et al.* (2000) tried to deplete the capacity of satellite cells to

replicate, by repeated cycles of atrophy and regrowth using three bouts of immobilization. They reported a significant loss in the proliferative potential of the resident satellite cells after just one bout of immobilization, whereas application of IGF-I increased this potential and rescued about 46% of the muscle mass. They suggested that, rather than the numbers or intrinsic defects of satellite cells in the old rats, it is the microenvironmental factors that are responsible for the impaired restorative ability of senile muscles (Chakravarthy *et al.*, 2000).

The mechanism underlying the limited proliferative potential of satellite cells is not thoroughly understood. One possibility that has been suggested is called “mitotic clock” which refers to the loss of some telomeric DNA each time a cell divides. Since telomeric DNA is not infinite, measuring the mean telomere length can be used to estimate the replicative potential of a human satellite cell population and this will in turn determine the regenerative potential of the muscle (Renault *et al.*, 2000). An enzyme called telomerase has been found to extend telomere sequences and could be a valid candidate for therapeutic use to preserve the satellite cell pool (Lundblad & Wright, 1996; Wright *et al.*, 1996; Di Donna *et al.*, 2000).

### ***Aging***

It has been reported that the number of muscle satellite cells is inversely proportional to chronological age (Renault *et al.*, 2002). This decrease in the proportion of satellite cells is not, however, constant over the life span of an

animal, but is sharpest during maturation and much slower from adulthood to senescence (Schultz & McCormick, 1994). Starting from 30% in the neonate, the proportion of satellite cells decreases with age to ~4% in adult muscles and ~2% in senescent muscles (Schultz & McCormick, 1994). Although this decrease is seen in all muscles, the mechanisms are different between oxidative and glycolytic muscles. In oxidative muscles such as *soleus*, the decrease in the relative number of satellite cells is brought about by an increase in the number of myonuclei while the absolute number of satellite cells remains constant. In a predominantly glycolytic muscle such as the *extensor digitorum longus*, the absolute number of satellite cells decreases with age as the number of myonuclei increases (Schultz, 1989).

Although the absolute number and proportion of satellite cells in a muscle decline with age, it does not seem to affect regenerative capacity. A cross-age transplantation study showed that the mass and maximum force of old muscles grafted into young hosts were not significantly different from those of young muscles grafted into the same young hosts. Conversely, young muscle grafted into old hosts regenerated no better than old muscles grafted into the same old hosts (Carlson & Faulkner, 1989). Carlson & Faulkner (1989) concluded that chronological age alone is not a factor that limits the intrinsic ability of a muscle to regenerate and that the poor regeneration of muscles in old animals is a function of the environment provided by the old host. Dedkov *et al* (2003b) suggested that aging does not repress the capacity of satellite cells to become activated and grow in the response to muscle denervation (Dedkov *et al.*, 2003b).

Furthermore, in another study using a low-frequency-stimulation model, Putman *et al.* (2001) found no difference between young and old rats in the contribution of satellite cells to allow fibre-type transition. It seems likely that satellite cells in old animals do retain part, if not all, of their intrinsic potential to contribute to muscle repair or modification.

In very old muscle the proportion of satellite cells relative to myonuclei can sometimes increase, particularly in animals affected with hindlimb neuropathy (Carlson *et al.*, 2001). This is probably due to the sporadic denervation associated with aging. It has been reported that there is a progressive loss in the number of motor axons supplying a muscle during aging (Booth *et al.*, 1994; Ishihara & Araki, 1988; Kadhiresan *et al.*, 1996; Larsson & Ansved, 1995), and this in turn results in denervation atrophy of the muscle and subsequent activation of satellite cells.

### ***Effects of Low-Dose Ionizing Irradiation***

Low dose  $\gamma$ -irradiation is a process that sterilizes the satellite cell population without damaging the muscle fibres (Wakeford *et al.*, 1991; Phelan & Gonyea, 1997). The energy from  $\gamma$ -irradiation disrupts hydrogen bonds of polynucleotides, causes multiple breaks in target DNA, and thus prevents satellite cell mitosis. Although some satellite cells attempt to divide after irradiation, mitotic failure and apoptosis predominate (Wheldon *et al.*, 1982; Wakeford *et al.*, 1991). Those irradiated satellite cells that remain in a quiescent state, appear to possess the capacity to repair their DNA, as evidenced by their



ability to begin to proliferate after exposure to a single 25-Gy dose of  $\gamma$ -irradiation (Mozdziak *et al.*, 1996). Because skeletal muscle fibres are post-mitotic, gene expression remains largely unaffected by low-dose  $\gamma$ -irradiation (Yang & Swenberg, 1991; Rosenblatt *et al.*, 1994; Phelan and Gonyea, 1997). It has been reported that only dosages between 120 and 180Gy damage skeletal muscle fibres (Lewis, 1954).

Rosenblatt & Parry (1992) stated that  $\gamma$ -irradiation sterilized satellite cells, caused “reproductive death” of satellite cells; this prevented compensatory hypertrophy of overloaded mouse muscle but allowed limited normal muscle growth (Rosenblatt *et al.*, 1994; Rosenblatt & Parry, 1993). This limited normal muscle growth, however, may be because DNA repair and mitotic recovery of satellite cells can still occur after a single dose of ionizing radiation (Mozdziak *et al.*, 1996; Gillies, 1987; Wakeford *et al.*, 1991; Quinlan *et al.*, 1995). It is proposed that after a single dose of irradiation some satellite cells could still undergo at least one mitotic division before their death (McGeachie *et al.*, 1993; Mozdziak *et al.*, 1996) and are still fusion-competent. However, Phelan and colleagues showed that a single 30-Gy  $\gamma$ -irradiation dose blocked the satellite cell activity in rat *soleus* for up to 4 weeks (Phelan & Gonyea, 1997). Collectively, the findings of these studies indicate a single low-dose of  $\gamma$ -irradiation is only partly effective in sterilizing the satellite cell population.

## **Part 2: Peripheral Nerve Injury**

### ***Morphological and Functional Changes***

If the nerve to a muscle is injured, either by transection or crush injury, the muscle will gradually waste over a period of weeks, which is termed denervation atrophy. This demonstrates that the muscle fibres are dependent on the motoneuron for the maintenance of their normal structure. The most obvious change in the muscle following denervation is a reduction in fibre size, as measured by fibre cross-sectional area. This atrophy can be detected at about the third day after denervation and is rapid in the following two months (Carlson, 1981; Dedkov *et al.*, 2001). Beyond this period, atrophy progresses at a much slower rate mainly because after two months of denervation the muscle has atrophied to 20% to 40% of its original mass, and a large portion of the muscle comprises connective tissues (Carlson, 1981; Sunderland & Ray, 1950). Accompanying this reduction of the muscle size, various fibre organelles such as the mitochondria and sarcoplasmic reticulum are also reduced in number or display atrophy (Stonnington & Engel, 1973).

Despite the process of muscle atrophy, embryonic fibres are formed during this process. In long-term denervated rat hindlimb muscles, the formation of new muscle fibres reached its maximum between two and four months following denervation and gradually decreased with progressive post denervation atrophy (Borisov *et al.*, 2001). However, most of the newly formed (regenerated) muscle fibres did not appear to undergo complete maturation, and morphologically they

resembled myotubes (Dedkov *et al.*, 2001). The regenerative process also frequently resulted in development of abnormal muscle cells that branched or formed small clusters (Dedkov *et al.*, 2001).

Lu *et al.*, (1997) & Dedkov *et al.* (2003a) reported that type II muscle fibres underwent more rapid atrophy compared to type I fibre. Although among different muscles, and between young and old rats, there is considerable variation in the response of different muscle fibre types to denervation. In surviving muscle fibres, sites of former motor end-plates remained identifiable and slow and fast types of myosin were also found (Dedkov *et al.*, 2001).

In addition to all the morphological changes described above, there are also significant changes in muscle function. As would be expected, the tension developed during a single twitch, or during tetanus, is reduced because the muscle undergoes denervation atrophy and loses mass rapidly (Fu & Gordon, 1995a). With prolonged denervation, there is a progressive decrease in the number of axons that reinnervate the muscle, which further contributes to the progressive decline in muscle force. In addition, the twitch becomes significantly slower and the duration of muscle fibre action potential following a single stimulus increases (Lewis, 1972).

### ***Cell and Nuclear Death***

As denervation progresses, a variable proportion of muscle fibres undergo further degenerative changes and may result in fibre death. The affected fibres and their nuclei swell and then begin to fragment. An interesting phenomenon is

that although nuclear death was seen in all types of muscle fibres after long term denervation, severely atrophic skeletal muscles continued to express developmentally and functionally important proteins, such as MyoD, myogenin, adult and embryonic subunits of the nicotinic acetylcholine receptor, and neural-cell adhesion molecule (NCAM) (Dedkov *et al.*, 2001). Furthermore, degeneration and death of myocytes occurred regardless of their size, which indicated that cell death in denervated muscles did not correlate with levels of muscle cell atrophy (Borisov *et al.*, 2001).

Although it would be expected that myogenesis is related to the severity of muscle fibre atrophy, this is actually not the case. A study showed the reactivation of myogenesis in the *tibialis anterior* and *extensor digitorum longus* muscles of the rat starts between days 10 to 21 following nerve transection, before atrophy has reached an advanced level, and long before dead cells are found in the tissue (Borisov *et al.*, 2001). The degree of atrophy and degenerative changes of individual fibres in denervated muscle is very variable. After prolonged denervation, myogenesis is a typical regenerative reaction that occurs mainly within the spaces surrounded by the basal lamina of dead muscle fibres (Borisov *et al.*, 2001).

### ***Reinnervation Capacity of Muscle***

. Although it is conceivable that the poor recovery of prolonged denervated muscle is due to the inability of the long-term denervated muscle to accept reinnervation, this does not seem to be the case. Each regenerated axon

reinnervated three to five fold more muscle fibres than normal (Fu & Gordon, 1995a; Ijkema-Paassen *et al.*, 2002). Fu & Gordon (1995) suggested that it is rather due to progressive deterioration of the intramuscular nerve sheaths, caused by regenerating axons growing outside the sheaths as an effect of prolonged denervation. An intrinsic factor causing muscle fibres to fail to fully recover their mass and cross-sectional area, even after the muscle is reinnervated, was also suggested (Fu & Gordon, 1995a). However, an earlier study showed full recovery of muscle weight after 7 months denervation followed by 10 months reinnervation in mice (Irintchev *et al.*, 1990), indicating that severe atrophy might be reversed if sufficient numbers of axons reach the muscle and no loss of muscle fibres had occurred.

### ***Reinnervation Capacity of Motor Nerve***

After peripheral nerve injury, either the motor nerve can regenerate and grow back to the muscle (direct reinnervation), or the surviving motor axons can sprout and establish synaptic connection with the denervated muscle (collateral reinnervation). In the first situation, the growing axon tips are guided down the columns formed with the Schwann cells of the stump, by factors such as laminin, fibronectin, neural-cell adhesion molecule (N-CAM) that can be found in the basement membranes of the Schwann cells. When the regenerating axons reach the denervated muscle, they are attracted by the molecular signals secreted from the old end-plate basement membrane to grow back to the former end-plate and form new neuromuscular junctions (Bennett *et al.*, 1973). This re-growth process does not occur at the same rate along the axon. Various studies

have shown different rates across species and at different sites of injury, but a common pattern is a faster rate at the proximal site and a slower rate near the distal part. In the second case, when the denervation has been incomplete and some motor axons have survived, sprouts can develop at several sites from the healthy axons, such as the nodes of Ranvier, the neuromuscular junction itself, or adjacent to it. These sprouts can then grow toward denervated muscle fibres in their vicinity and form new neuromuscular junctions.

If reinnervation starts and progresses right after the injury, a return of muscle function can be expected. Conversely, when reinnervation is delayed, it will be less successful and can result in a malfunction of the muscle. The primary cause of the poor recovery after long-term denervation has been suggested to be a profound reduction in the number of axons that successfully regenerate through the deteriorating intramuscular nerve sheaths (Fu & Gordon, 1995a).

### ***Satellite Cell Activation and Depletion***

A number of laboratories have reported that the proportion of satellite cells increases during the initial period following denervation (Viguie *et al.*, 1997; McGeachie, 1989). During the first 2 months of denervation, activated satellite cells form new myotubes on live differentiated muscle fibres. At two and four months, satellite cells still showed signs of activation, such as elongated cytoplasmic processes, an increased concentration of cytoplasmic organelles, and basal lamina material was deposited between the satellite cells and muscle fibres (Lu *et al.*, 1997). As denervation progressed, activated satellite cells

became more widely separated from their associated muscle fibres. Some satellite cells even broke free from their muscle fibres, and others acted as bridges between two muscle fibres (Lu *et al.*, 1997). These findings showed that satellite cells were enormously activated post denervation, in turn supporting the idea that reversal of denervation atrophy by reinnervation depends on satellite cell availability for incorporation of new nuclei.

The number of satellite cells is significantly reduced in long-term denervated muscles, as compared with age-matched control muscles. In 25-month denervated rat muscle, satellite cells were only attached to existing muscle fibres, but were not seen on newly formed fibres (Dedkov *et al.*, 2001). It was further suggested that the absence of satellite cells in a population of immature newly formed muscle fibres that had arisen as a result of continuous reparative myogenesis may be a crucial, although not necessarily the only, factor underlying the poor regenerative ability of long-term denervated muscle (Dedkov *et al.*, 2001). An *in vitro* study further showed that skeletal muscle denervation increases satellite cell susceptibility to apoptotic cell death (Jejurikar *et al.*, 2002) as evidenced by the increase of caspases, a family of intracellular proteolytic enzymes known to be components of an apoptosis cascade. It is conceivable that this apoptotic process may partially contribute to the loss of satellite cells seen in denervated muscles.

Since the interval between denervation and the arrival of regenerating nerve fibres at a denervated muscle is crucial for motor recovery, it was postulated that prolonged denervation may result in a reduction in a muscle fibres' ability to

respond to the influence of the motor nerve. In this regard, efforts have been made to enhance muscle fibres' intrinsic ability to recover by cell therapy. Lazerges and colleagues (2004) transplanted satellite cells into cardiotoxin-induced degenerating muscles which were previously denervated. They found that the transplantation of primary satellite cells significantly improved the recovery of skeletal muscles that had become reinnervated compared with muscles that were still denervated (Lazerges *et al.*, 2004). These results suggest that cell transplantation has a potential for muscle repair, providing that the muscle is normally innervated.



## CHAPTER III: METHODS

### **Part 1: Experimental Model**

#### ***Animals***

Twenty-four adult female Sprague-Dawley rats were obtained from the local animal facility at the University of Alberta and used in this study (age 4 months old). The rats were treated in accordance with the guidelines of the Canadian Council for Animal Care and the study received ethical approval from the University of Alberta. The rats were housed in a thermally controlled room maintained at 22°C with 12-hour dark cycles alternated with 12-hour light cycles and received standard rat chow and water *ad libitum*. After a week of adjustment to the new environment, the rats were randomly assigned to a nerve crush (n=12) or nerve crush with irradiation (n=12) group.

#### ***Repeated Nerve Crush Injury***

In all groups, the *common peroneal* nerve of the left leg was repeatedly and sequentially crushed 5, 10, 15 and 20 mm proximal to the anterior leg compartment on days 0, 7, 21, and 42 of this study (Figure 3-1). The time point used here was based on a pilot study showing that reinnervation occurred 7 days later after a crush at a position 5 mm proximal to the anterior leg compartment. The right leg of each rat served as an internal control. For all surgeries, the animals were deeply anesthetized with a combination of ketamine (60mg/kg body

weight) and xylezene (8mg/kg body weight). The skin of the left hindlimb was shaved and disinfected with iodine solution. An incision in the skin was made from the knee to approximately 1cm below the superior-lateral aspect of the anterior crural region, superficial to the *common peroneal* nerve. The *common peroneal* nerve was then exposed by an incision that separated the fascia between the *tibialis anterior* and *gastrocnemius* muscles. Using the tips of a #5 Dumont forceps (Fine Science Tools, North Vancouver, B.C., Canada), the *common peroneal* nerve was crushed 5, 10, 15 or 20 mm proximal to the anterior leg compartment for 5 seconds. The crush injury was confirmed by observing a clear translucent break on the white nerve, which was approximately 1mm in width. The skin was then sutured with 4-0 sterile silk.

### ***Gamma ( $\gamma$ )-Irradiation Treatment***

In the nerve crush and radiation group, focal application of  $\gamma$ -irradiation to muscles of the anterior leg compartment was given on days 70, 98 and 126 to prevent satellite cell proliferation and fusion during the major phase of muscle regeneration (Figure 3-1). This was done by exposure to a  $^{137}\text{Cs}$  source using the Gamma Cell-40 Irradiation Unit (Health Services Laboratory Animal Services (HSLAS), Heritage Medical Sciences Building, University of Alberta), under sodium pentobarbital (45mg/kg) induced anesthesia. The left anterior crural compartment was exposed to 30 Gy of  $\gamma$ -radiation (Phelan & Gonyea, 1997; Rosenblatt & Parry, 1992; Rosenblatt & Parry, 1993; Rosenblatt *et al.*, 1994), while the remainder of the animal was shielded with 2.5cm thick lead from both above and below to prevent sterilization of stem cells within other tissues.

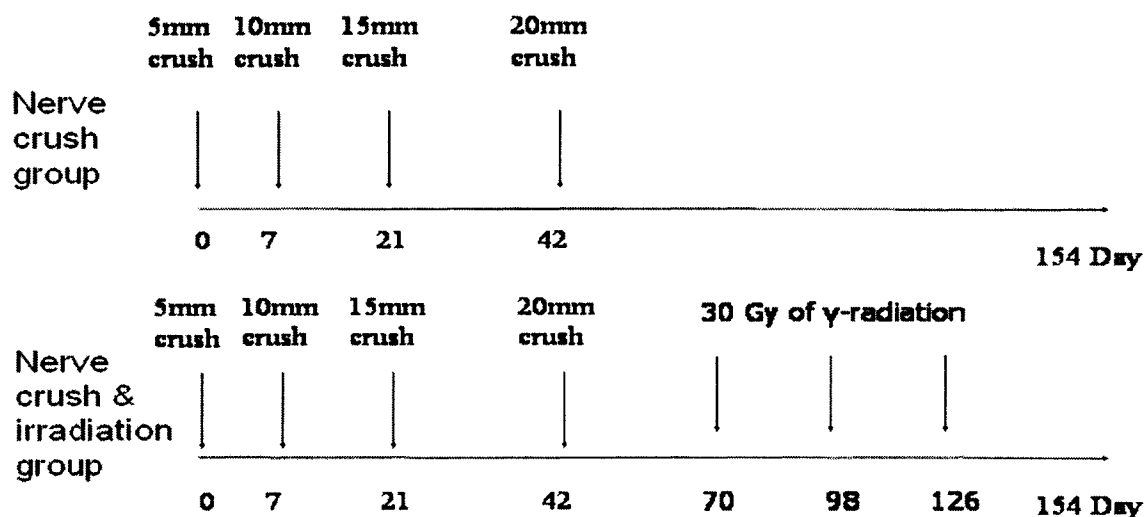


**Figure 3-1.** Summary of the experimental design.

### ***Muscle Sample Preparation***

Upon completion of the study (day 154), rats were sedated and isometric measurements were completed as outlined below. Animals were subsequently euthanized with an overdose of sodium pentobarbital (100mg/kg body mass). The *tibialis anterior* muscles were immediately excised and frozen in melting isopentane (-156°C) and stored in liquid nitrogen (-196°C) for later immunocytochemical and biochemical analyses.

*Tibialis anterior* muscles of the left leg and right leg were transversely sectioned at the mid-belly under -20°C conditions and mounted in embedding medium (Tissue-Tek O.C.T. Compound, Miles Scientific, USA). A series of 10- $\mu$ m-thick sections were cut using a freezing microtome (-20°C), mounted onto poly-L-lysine coated slides (Cedarlane Laboratories, Hornby, ON, Canada) and

stored at -80°C until used for immunohistochemical staining. A secondary series of 16- $\mu$ m-thick sections was also prepared in the same manner and used for myogenin, PCNA, M-cadherin, and collagen and laminin staining.

## **Part 2: Analyses**

### ***Functional Measurements***

In the final acute experiment, the rats were anesthetized with sodium pentobarbital (45mg/kg), the brachial vein was cannulated for additional injections of anesthetic (1% of the initial dose) to maintain deep anesthesia, and the rats were intubated with a tracheal cannula for artificial ventilation if required. A laminectomy was performed to expose the L4 and L5 ventral roots. All muscles other than *tibialis anterior* in the hindlimb were denervated by section of their nerve supply. The *tibialis anterior* muscle was exposed in both hindlimbs and, as far as possible, freed from other muscles and connective tissues. Care was taken to keep the blood supply intact. The distal muscle tendon was tied with a 2-0 silk suture and secured to a force transducer (KH-102A, Kulite Semiconductor Products, Leonia, NJ, U.S.A.) for single MU force measurements. The bare ends (~ 5 mm) of two Teflon-coated fine silver wires (75  $\mu$ m), inserted into the *adductor femoris* and *semimembranous* muscles ~ 10 mm apart longitudinally on either side of the sciatic nerve, were used to stimulate the sciatic nerve. The wire was threaded into a 27-gauge needle, and the bared end was coiled around the needle. Intramuscular insertion of the needle left a coil of bare wire that was very stable and highly effective as a stimulating electrode. Rats

were placed prone on a heating pad, mounted on a stereotaxic frame, and secured with clamps at the knees and ankles. The skin surrounding the laminectomy was drawn up to form a pool, which was filled with human grade mineral oil maintained at 34°C. Rectal temperature was maintained at 37°C (Totosy de Zepetnek *et al.*, 1992b; Rafuse *et al.*, 1992; Gordon & Stein, 1985; Rafuse & Gordon, 1996a; Rafuse & Gordon, 1996b).

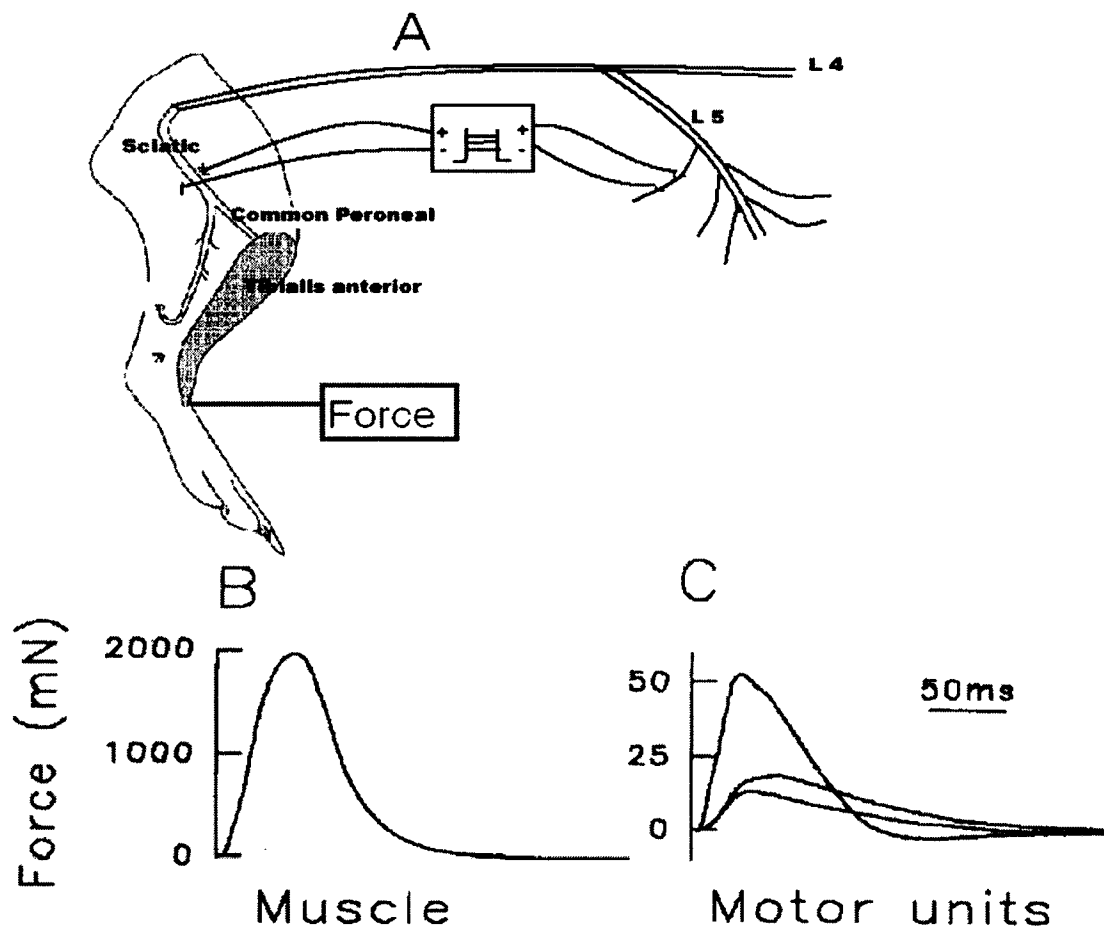


**Figure 3-2.** Schematic representation of whole muscle and motor unit twitch force recordings. (A) *Tibialis anterior* muscles were isolated by denervating all other hindlimb muscles and attached to a force transducer. Ventral roots L4-L5 were isolated and split for stimulation of single motor axons contributing to *tibialis anterior* muscle; (B) Twitch contraction of the whole muscle was elicited by maximal nerve stimulation; (C) ventral root filaments were teased so that stimulation elicited all-or-none increments of force in the *tibialis anterior* muscle.

Single *tibialis anterior* muscle motor units were functionally isolated by stimulating fine filaments dissected from the L5 ventral root. All-or-none firing at threshold stimulation was carefully checked for several minutes to ensure that a single unit was isolated. A second criterion for unit isolation required no change in force amplitude and shape (Totosy de Zepetnek *et al.*, 1992b; Rafuse *et al.*, 1992; Gordon & Stein, 1985; Rafuse & Gordon, 1996a; Rafuse & Gordon, 1996b). The method used to calculate the number of motor units is illustrated in Figure 3-2: twitch contractions of three individual motor units were obtained by digital subtraction (Figure 3-2, C); the total number of motor units in each muscle was calculated by dividing muscle twitch force (Figure 3-2, B) by the mean motor units twitch force. For example, when muscle twitch force is 1990 mN and the mean motor units twitch force is 14 mN, the calculated motor units number should be 142 (Fu & Gordon, 1995b).

Isometric muscle function measures were completed according to Tam *et al.* (2001). Before each series of recordings, the optimal resting length ( $L_0$ ) required to generate maximum force was determined for each muscle. Maximum twitch (TW: mN) and tetanic forces (TET: mN) were sequentially recorded in the right and left *tibialis anterior* muscles. TW was determined as the average of peak forces generated by five individual twitches elicited at 1 Hz. Time-to-peak tension (TTP, ms) was determined as the time elapsed from time 0 to peak force production. The half-rise time (1/2RT: ms) was calculated as the time from the onset of contraction to 50% of the maximum force produced. The half-fall time (1/2FT: ms) was recorded as the time required for the twitch peak force to decay

by 50%. The presence of whole muscle 'sag' was calculated as the ratio of final-to-initial force generated from an unfused tetanic contraction using an interval of  $1.25 \times \text{TTP}$  for 800 ms. The sag ratio has been used to classify single motor units as "slow" if the ratio is  $\geq 1.0$  or "fast" if the ratio is  $< 1.0$ . TET was determined as the force produced by 21 pulses (100 Hz) given at an interstimulus interval of one-third of the muscle contraction time (Totosy de Zepetnek *et al.*, 1992b; Gordon & Stein, 1985). All measurements were amplified, viewed on an oscilloscope, digitized using Axoscope and stored on disks. The force recordings were later analyzed using Clampfit (Axon Instruments).

### **Antibodies**

Monoclonal antibodies (MAbs), harvested from hybridoma cell lines (American Type Culture Collection, Manassas, VA, U.S.A.), were used to examine changes in muscle fibre type distribution: BA-D5 (IgG, anti-MHC I $\beta$ ), SC-71 (IgG, anti-MHC IIa), BF-F3 (IgM, anti-MHC IIb) and BF-35 (IgG, anti-MHC (recognizes all MHC except IId/x)) (Schiaffino *et al.*, 1989). Type-I $\beta$ , -IIA, and -IIB fibres were identified by positive staining of fibres, while type-IID/X fibres were identified by the absence of staining. Developmental (embryonic) MHC-embryonic was detected immunohistochemically with the monoclonal anti-MHC embryonic (clone BF-45) (Schiaffino *et al.*, 1988).

Changes in total myonuclear content were evaluated using Harris' Hematoxylin with Eosin stain. Satellite cell contents were analyzed immunohistochemically using rabbit polyclonal anti-myogenin antibody (IgG, M-

225), goat polyclonal M-cadherin (IgG, N-19) (Santa Cruz Biochemical, CA, U.S.A.) and mouse monoclonal anti-PCNA (IgG, clone PC10) (Serotec, Oxford, UK). Mouse monoclonal anti-dystrophin antibody directed against the carboxy terminus (DYS2) was obtained from Novocastra Laboratories (Newcastle, UK). Rabbit polyclonal anti-laminin was obtained from ICN Biomedicals (Costa Mesa, CA, U.S.A.). Mouse monoclonal anti-desmin (clone DE-U-10) and anti-vimentin (clone V9) were obtained from Sigma (St. Louis, MO, U.S.A.). Nerve regeneration, reinnervation and establishment of motor endplates were determined by immunofluorescent staining with rabbit polyclonal anti-NCAM (Chemicon International, Inc., Temecula, CA, U.S.A.).

Biotinylated horse-anti-mouse IgG (BA-2001), biotinylated goat-anti-rabbit IgG (BA-1000), biotinylated horse-anti-goat IgG (BA-9500), and biotinylated goat-anti-mouse IgM (BA-2020) were obtained from Vector Laboratories (Burlingame, CA, U.S.A.). Fluorescein isothiocyanate (FITC) conjugated donkey anti-rabbit IgG (Jackson Immuno Research Laboratory, West Grove, PA, U.S.A.) was used for NCAM staining. Nonspecific control mouse IgG antibodies were obtained from Santa Cruz Biochemical.

***Immunohistochemistry for Myosin Heavy Chain Isoforms, Desmin, Vimentin, and Dystrophin***

10- $\mu$ m-thick frozen sections were air-dried for 30 min. Sections were then washed once in PBS-Tween (0.1% (v/v) Tween-20, pH 7.4), twice in PBS (pH 7.4), and incubated for 15 min with 3% (v/v) H<sub>2</sub>O<sub>2</sub> in methanol. Blocking



solutions were prepared in PBS-tween with 2.4% (v/v) bovine serum albumin (BSA) and 6% (v/v) horse (BS-1) or goat serum (BS-2). Sections were washed and incubated for 1 h in a mixture of Avidin D blocking solution (Vector Laboratories Inc, Burlingame, CA, U.S.A.) and BS-1 except for BF-F3, which used BS-2. Excess blocking solution was removed, and the primary MAb was overlaid and incubated overnight at 4°C. Primary antibodies were diluted in the mixture of Biotin blocking solution (Vector Laboratories) and BS-1 or BS-2 (BF-F3) as follows: SC-71 1:100, BF-45 1:50, BA-D5 1:400, BF-F3 1:400, BF-35 1:10,000, dystrophin 1:10, desmin 1:100, vimentin 1:25. Control sections were completed in parallel in which (a) the primary antibody was substituted with a nonspecific control mouse IgG (1:2000), or (b) the primary antibody was omitted. Sections were washed as before and biotinylated horse-anti-mouse-IgG (SC-71, BF-45, BA-D5, BF-35) or biotinylated goat-anti-mouse-IgM (BF-F3), were applied at a dilution of 1:400 in BS-1 or BS-2 (BF-F3). For dystrophin, desmin, and vimentin, the dilution factor for the secondary antibodies was adjusted to 1:200. After several washings, sections were incubated with Vectastain ABC (avidin-biotin Horse Radish Peroxidase complex) reagent (Vector Laboratories) diluted in PBS for 1 h. Sections were washed as before and reacted with substrate solution (DAB/NiCl<sub>2</sub>) (Vector Laboratories) for various durations as follows: 8 min for controls, SC-71, BF-45, BA-D5, BF-35, and BF-F3; 6 min for desmin; 5 min for dystrophin and vimentin. Reactions were stopped by washing several times with distilled water. Stained sections were subsequently dehydrated in ethanol, cleared with xylene and mounted with Entellan (Merck, Darmstadt, Germany).

### ***Immunohistochemistry for Collagen IV with Laminin, PCNA, M-cadherin and Myogenin***

16  $\mu\text{m}$  thick frozen sections were air dried and fixed for 10 min in cold acetone ( $-20^{\circ}\text{C}$ ), excess acetone was then allowed to evaporate. No fixation was used for collagen IV plus laminin staining. Sections were then treated as previously described with the following modifications. Primary antibodies were diluted as follows: collagen IV with laminin 1:100 in BS-2; PCNA 1:100 in BS-1; M-cadherin 1:1:50 in BS-1; and myogenin 1:100 in BS-2. The dilution factor for secondary antibodies was 1:200 and the following were used: biotinylated goat-anti-rabbit-IgG in BS-2 (myogenin; collagen IV with laminin), horse-anti-goat-IgG in BS-1 (anti-M-cadherin) or horse-anti-mouse-IgG in BS-1 (PCNA). Sections were reacted with substrate for various durations: 8 min for collagen IV with laminin and PCNA, 6 min for M-cadherin and 3 min for myogenin.

### ***Immunohistochemistry for NCAM***

16  $\mu\text{m}$  thick frozen sections were air dried and then fixed for 5 minutes in cold methanol ( $-10^{\circ}\text{C}$ ); excess methanol was allowed to evaporate. Sections were incubated with normal donkey serum, diluted 1:20 in PBS, for 1 hr at room temperature and then washed in PBS. Primary antibody was diluted (1:100) in PBS with 10% (v/v) BSA, overlaid and incubated overnight at room temperature. Slides were rinsed in PBS and incubated in dark with FITC labeled secondary antibody (diluted in PBS 1:100) for 1 hr at room temperature. Stained sections

were rinsed in PBS, distilled water, and subsequently air dried and mounted with cyto seal.

### ***Harris' Haematoxylin with Eosin Stain***

10  $\mu\text{m}$  thick frozen sections were air dried and then fixed for 10 min in cold acetone ( $-10^{\circ}\text{C}$ ); excess acetone was then allowed to evaporate. Sections were incubated with Harris' Haematoxylin (Fisher Scientific, Ottawa, Ontario, Canada) for 8 min and rinsed in distilled water. Sections were then differentiated in acid alcohol (1000ml alcohol and 10ml HCl) for 8 sec and rinsed as before, and then blued in 1% (v/v) sodium bicarbonate for approximately 2 min. After washing in running tap water for 5 min, sections were counterstained with Eosin Y/Phloxine (Sigma) solution for 15 sec and rinsed again. Stained sections were subsequently dehydrated in ethanol, cleared with xylene and mounted with Entellan.

### ***Morphometric Fibre Analyses***

MHC-based fibre type analysis was completed with a Leitz Diaplan microscope (Enrst Leitz Wetzlar GmbH, Germany) fitted with a Pro Series High Performance CCD camera (Media Cybernetics, USA) and analytical imaging software programs (Image Pro Plus 4.0). Using a custom designed software program (Putman *et al.*, 2000), three separate regions (deep, middle, and superficial) were analyzed in each muscle from nerve crush with irradiation (total fibres:  $624 \pm 20$  fibres/muscle), nerve crush with irradiation contralateral control (total fibres:  $417 \pm 22$  fibres/muscle), nerve crush (total fibres:  $706 \pm 22$

fibres/muscle), and nerve crush contralateral control (total fibres:  $459 \pm 18$  fibres/muscle) legs. A total of 26,472 fibres were examined for fibre cross-sectional area analyses. Briefly, images of stained cross sections were automatically outlined using the computer, and the enclosed area was determined from the number of pixels within each outlined fibre. The camera was calibrated with a known object, and a correction factor of 0.6241 was established. The fibre type distribution was performed on the same fibres. Fibres stained dark for both MHC-I and MHCIIa, were classified as type I/IIA hybrid fibres. Fibres were identified as type IID(X)/B mixed fibres when the staining was lighter than normal stained type IIB fibres and was stained light after BF-35 antibody was applied. The cross-sectional areas examined for satellite cells (M-cadherin), proliferating satellite cells (PCNA), terminally differentiating satellite cell progeny (myogenin), and total intrafibre myonuclei (Harris' Hematoxylin with Eosin) were 1.36, 6.8, 2.04 and 1.36 mm<sup>2</sup> per muscle cross-section, respectively.

### ***Electrophoretic Analyses of MHC Isoforms***

Myosin heavy chain isoform electrophoretic analyses were completed according to previously published procedures (Hamalainen & Pette, 1996; Naumann & Pette, 1994; Hansen *et al.*, 2004; Putman *et al.*, 2004). Muscles were pulverized under liquid nitrogen and crude myosin extracted in a solution containing 300 mM KCL, 100 mM sodium pyrophosphate. Briefly, muscle samples were homogenized in 6 volumes of a buffer containing 100 mM Na<sub>4</sub>P<sub>2</sub>O<sub>7</sub> (pH 8.5), 5 mM EGTA, 5 mM MgCl<sub>2</sub>, 0.3 M KCl, 10 mM DTT and 5 mg/ml of a

protease inhibitor cocktail (Complete TM, Roche Diagnostic, Germany). Homogenates were stirred for 30 min on ice and centrifuged at 12,000xg for 5 min at 4°C. The supernatant was subsequently diluted 1:1 with glycerol, followed by protein determination using Bradford Protein Assay (Bradford, 1976). Extracts were subsequently stored at -20°C until analyzed. Prior to gel loading, muscle extracts were diluted in laemmli-lysis buffer and bromophenol blue-sucrose solution (Naumann & Pette, 1994) so that the final concentration of protein in each sample was 0.15 mg/ml. After dilution, the samples were heated to 100 °C for 5 min. An alkylation step was performed by adding 10 µl 20% (v/v) iodoacetamide per 100 µl of sample followed by incubation for 30 min at room temperature. After incubation, samples were centrifuged at 12,000xg at 21°C for 5 min and the supernatant retained for analysis. MHC isoforms were then separated electrophoretically on 7% (v/v) separating gels containing 35% (v/v) glycerol under denaturing conditions. One mg of total protein was loaded per lane and electrophoresed for 24 hr at 275 V at 10°C. Gels were subsequently silver stained (Oakley *et al.*, 1980) and evaluated by densitometry (SynGene ChemiGenius, GeneTools, SynGene, U.K.)

### ***Statistical Analyses***

Data are presented as means  $\pm$  SEM. Differences between treated muscles and contralateral control were assessed using a Two-Way Analysis of Variance with rat as the unit of measurement. When a significant *F*-ratio was found, differences were located using the LSD post-hoc analysis for *planned comparisons*. Because in some cases the control values differed between

groups, the absolute differences between treated muscles and the respective contralateral controls were analyzed by a two-tailed independent Student's t-test.

Differences were considered significant at  $P < 0.05$ .

## CHAPTER IV: RESULTS

### Functional Measures

Repeated nerve crush injury caused a significant decrease in muscle mass (Table 4-1) even after the muscle was reinnervated. Irradiation significantly reduced the number of motor units by ~28% within the nerve crushed muscle, which corresponded to a 17% increase in motor unit size (Table 4-2). Muscle mass and force recovered to similar degrees in both groups (Table 4-1 and 4-2). The twitch and tetanic force of the crushed muscles were lower than the contralateral controls (Figure 4-1 A, E). The TTP (Figure 4-1 B) and 1/2RT (Figure 4-1 C) were reduced only in the irradiated nerve crushed muscle, whereas 1/2FT (Figure 4-1 D) and SAG ratio (Figure 4-1 F) were not different between nerve crushed and control muscles. Changes of the treated muscles, relative to their respective contralateral controls, were not different between irradiated and non-irradiated groups (Figure 4-2).

### Reinnervation

Figure 4-3 shows that reinnervation reached a level close to normal conditions in both groups. NCAM positive staining was found at the neuromuscular junctions in normally innervated muscles and around denervated muscle fibres.

### **Myonuclear Content and Satellite Cell Activity**

Representative photomicrographs of myonuclei are shown in Figure 4-4. The Harris' Haematoxylin & Eosin staining was used to evaluate the total myonuclei content (A); the staining of myogenin was used to detect satellite cell progeny that had committed to or were in the later stages of terminal differentiation (B); quiescent satellite cells were identified by M-cadherin staining (C) and PCNA recognized proliferating cells in the S phase of their cell cycle (D).

The absolute number of total myonuclei, differentiated and quiescent satellite cells were all increased in treated muscles compared to their contralateral controls (Figure 4-5 A, B, C), whereas proliferating cells were only increased in the non-irradiated treated muscle (Figure 4-5 D). After corrected for changes in cross-sectional areas, total myonuclei, quiescent satellite cells and proliferating cells were all decreased in treated muscles compared to their contralateral controls (Figure 4-6 A, C, D), whereas satellite cells in their late differentiation and fusion states were not changed (Figure 4-6 B). Changes of the treated muscles relative to their respective contralateral control were not different between irradiated and non-irradiated group (Figure 4-7).

### **Fibre Cross-sectional area**

Fibre cross-sectional area was analyzed by immunohistochemical staining of each type of fibre (Figure 4-8). For all four fibre types, the fibre cross-sectional areas were reduced in treated muscles (Figure 4-9). When hybrid fibres were



examined, a larger area of type I & IIA hybrid fibre was seen in the nerve crushed muscles (Figure 4-10 B). Changes of the treated muscles relative to their respective contralateral control were not different between the irradiated and non-irradiated group (Figure 4-11, 12).

### **Fibre Type Transitions**

When using immunohistochemistry (Figure 4-8) to analyze fibre type distribution (Figure 4-13), there were no differences in the proportion of type I fibres between groups. Type IIA and IID(X) fibres were increased in non-irradiated treated muscles, whereas only type IIA fibres were elevated in irradiated treated muscles. Both treated muscles displayed fewer type IIB fibres. Hybrid fibres were also analyzed separately (Figure 4-14), which showed an additional increase in type I/IIA fibres(B) and no change in the proportion of type IIA fibres (C) in non-irradiated treated muscles. Greater type IID(X) (Figure 4-15 C) and lower type IIB fibre (Figure 4-15 D) proportion were found in the non-irradiated group compared with the irradiated group (Figure 4-15). These changes remained when hybrid fibres were analyzed separately (Figure 4-16).

Fibre type transition was also evaluated using SDS-PAGE technique (Figure 4-17). The results showed similar increases in MHC IIa and MHC IIc and a similar decrease in MHC IIb in both groups (Figure 4-18-B, C and D). Changes of the treated muscles relative to their respective contralateral control were not different between the irradiated and non-irradiated groups (Figure 4-19).

**Table 4-1:** Body mass, muscle mass, and crushed-to-control muscle mass ratio of rat *tibialis anterior*

Condition	Leg	Muscle Mass (mg)	Crushed-to-Control Muscle Mass Ratio (%)	Body Mass (g)
Non-irradiated	Control	692.4 ± 16.36 *	73.4 ± 2.46	443.4 ± 16.12
	Crushed	506.0 ± 15.77		
Irradiated	Control	726.2 ± 21.59 *	72.5 ± 1.21	424.4 ± 13.68
	Crushed	524.3 ± 11.82		

Data are means ± SEM. "\*" indicates Crushed is significantly different from Control within a treatment condition,  $P < 0.05$ .

**Table 4-2:** Muscle mean motor unit twitch force, motor unit number and crushed-to-control muscle twitch ratio of rat *tibialis anterior*

Condition	Mean Motor Unit Twitch Force (mN)	Motor Unit Number	Crushed-to-Control Twitch Ratio (%)
Non-irradiated	12.6 ± 0.89 *	146.3 ± 14.87 *	53.3 ± 2.97
Irradiated	17.1 ± 1.47	102.2 ± 9.45	54.7 ± 1.34

Data are means ± SEM. "\*" indicates Non-irradiated is significantly different from Irradiated, P < 0.05.

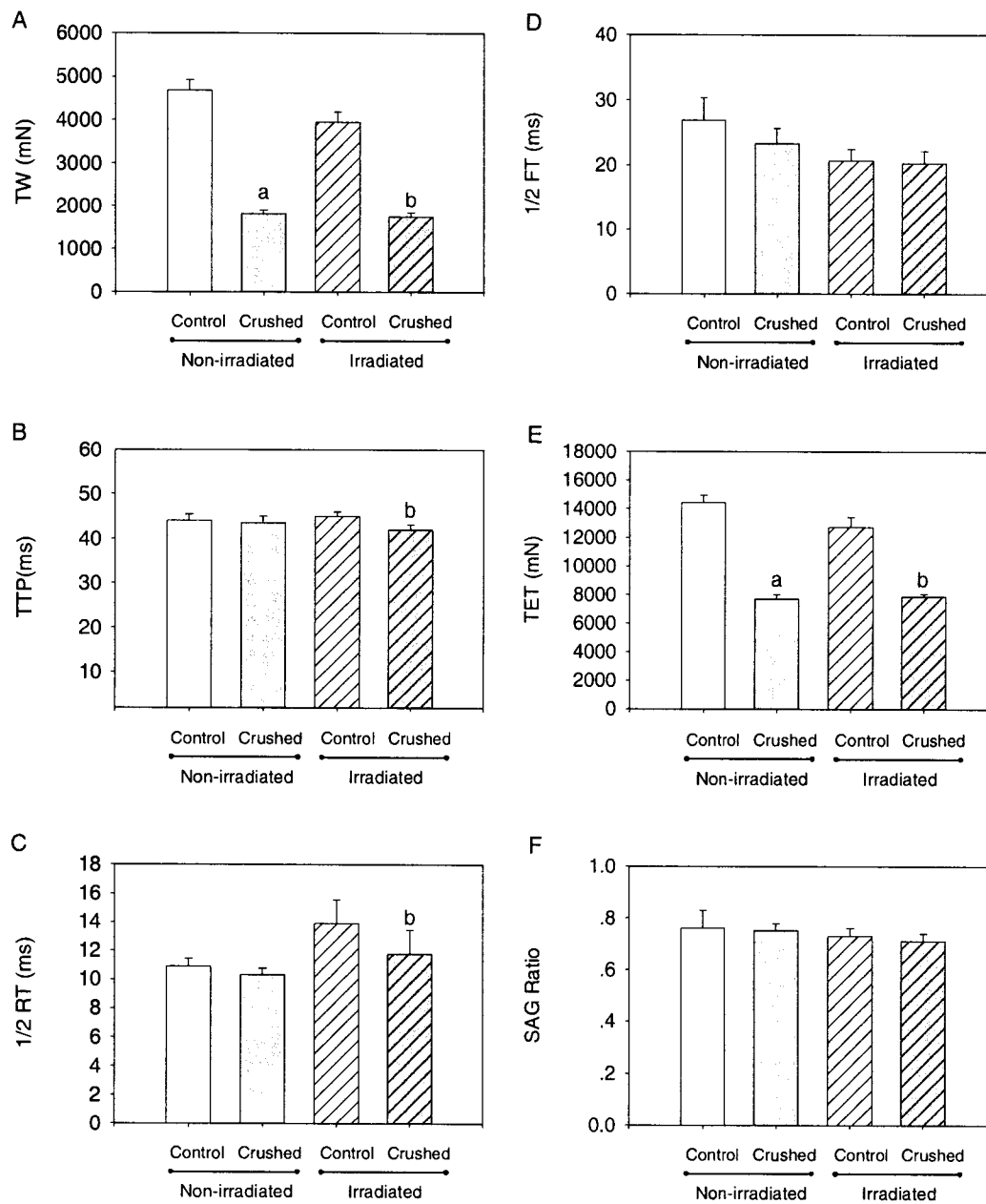


**Figure 4-1.** Isometric functional properties of *tibialis anterior* muscles: (A) twitch force; (B) time to peak force; (C) half force rise time; (D) half force fall time; (E) tetanus force; (F) SAG ratio. "a" and "b" indicate significant differences at  $P < 0.05$ . a: non-irradiated nerve crushed muscle vs. contralateral control; b: irradiated nerve crushed muscle vs. contralateral control.

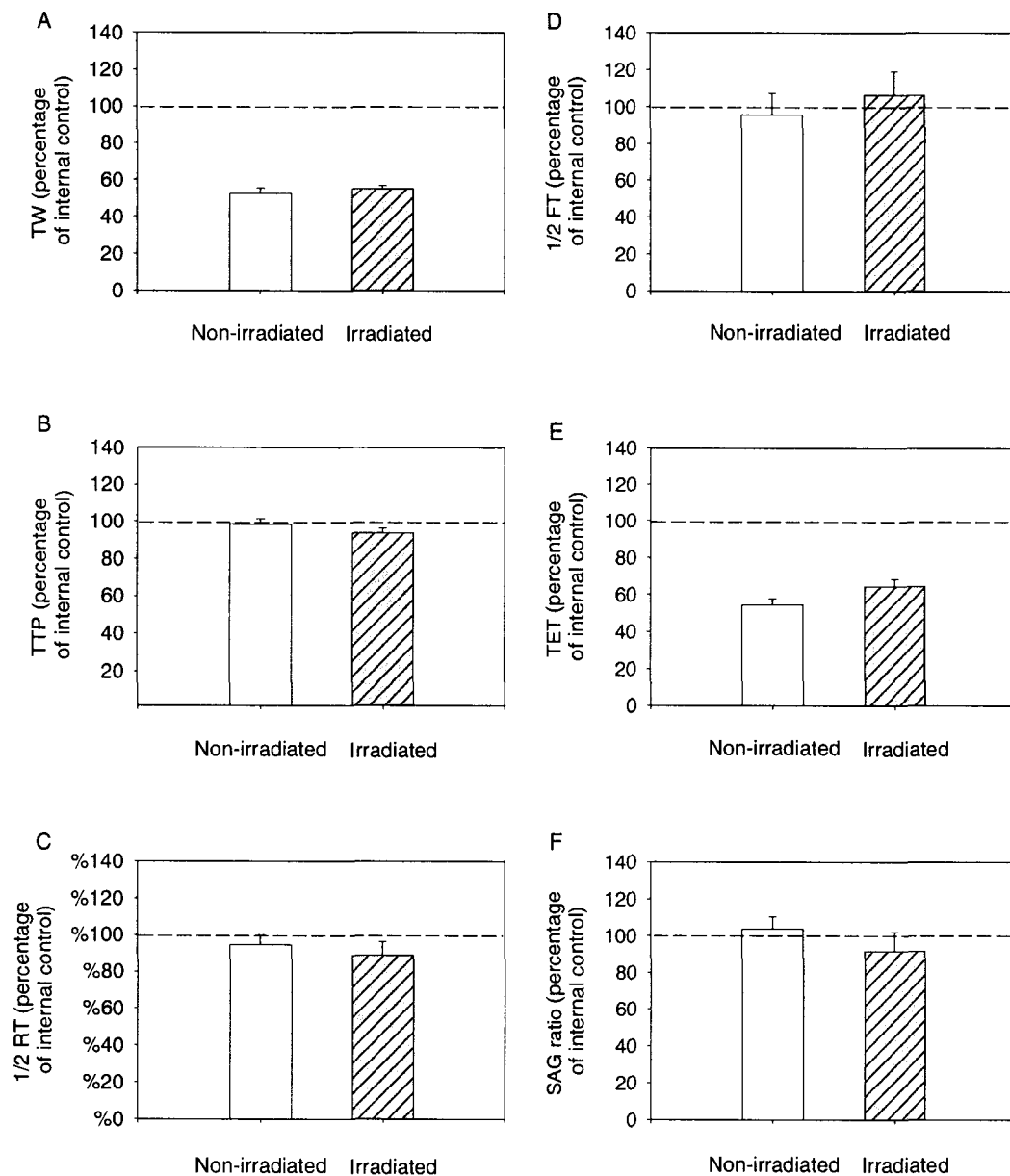


**Figure 4-2.** Changes in the isometric functional properties of the treated *tibialis anterior* muscles relative to their respective contralateral controls. The values of contralateral controls are 100%. Data are calculated from those displayed in Figure 4-1. (A) twitch force; (B) time to peak force; (C) half force rise time; (D) half force fall time; (E) tetanus force; (F) SAG ratio.

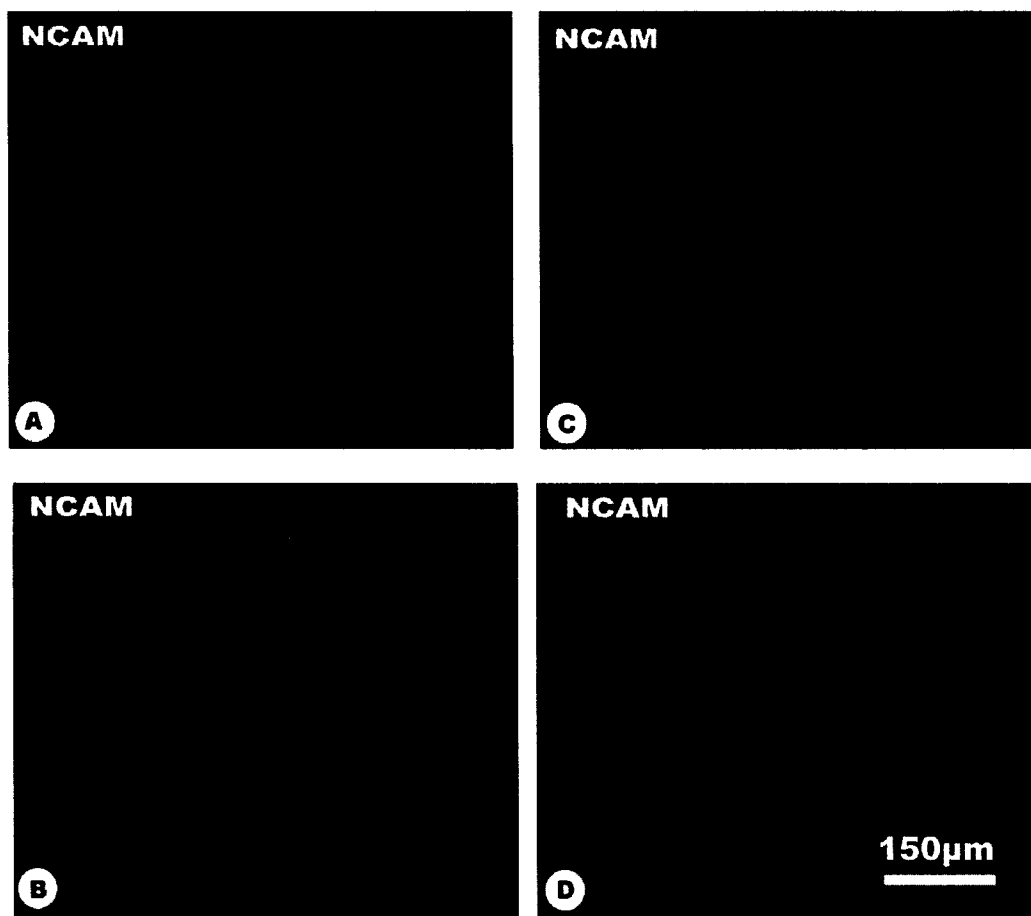


**Figure 4-3.** Representative NCAM stains of *tibialis anterior* muscles: (A) contralateral control of nerve crushed *tibialis anterior* muscle; (B) contralateral control of irradiated & nerve crushed *tibialis anterior* muscle; (C) nerve crushed *tibialis anterior* muscle; (D) irradiated & nerve crushed *tibialis anterior* muscle.

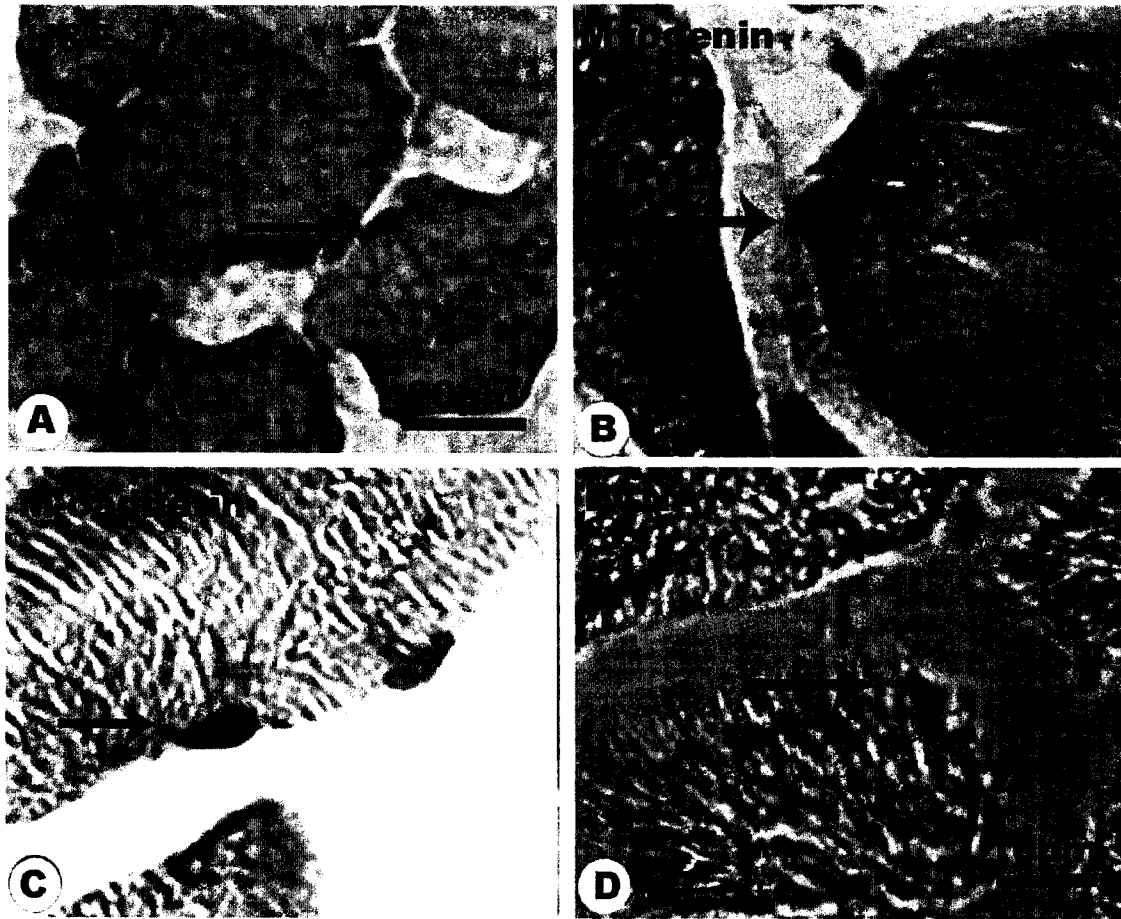


**Figure 4-4.** Representative photomicrographs of (A) H&E, (B) myogenin, (C) M-cadherin and (D) PCNA staining. Arrowheads indicate positively stained nuclei. Bar in D applies to B and C.

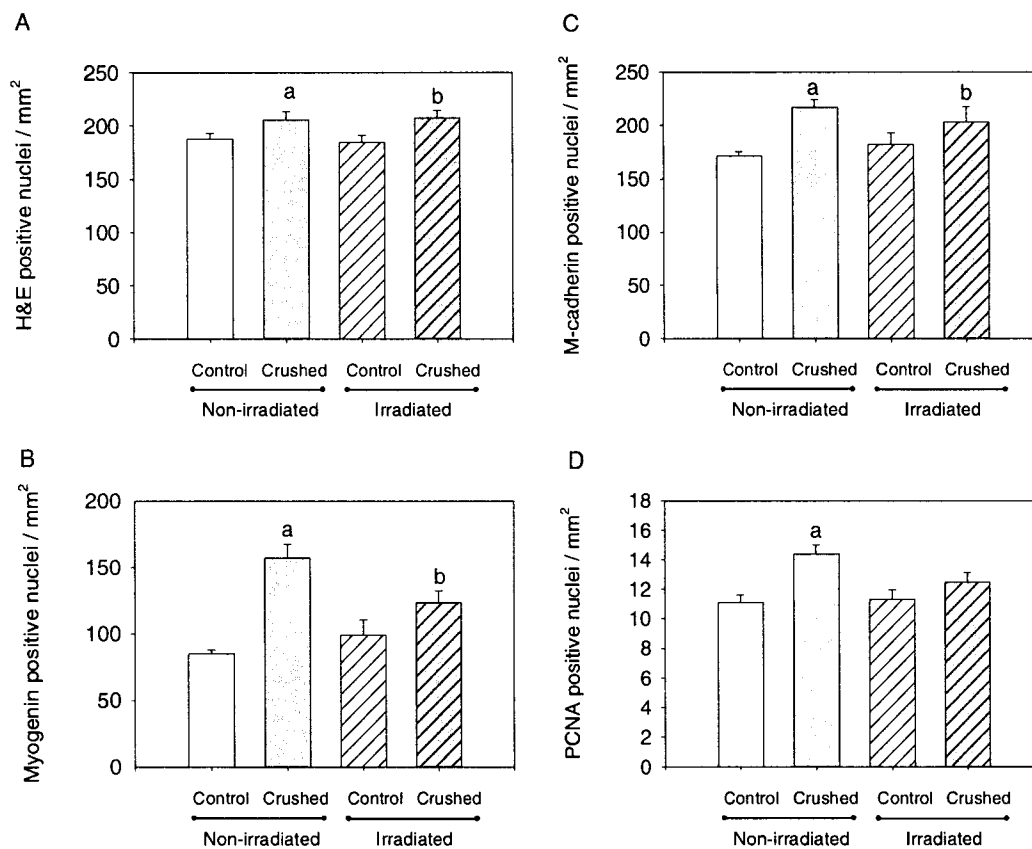


**Figure 4-5.** Positively stained myonuclei number per mm<sup>2</sup> (A) H&E, (B) myogenin, (C) M-cadherin and (D) PCNA. “a” and “b” indicate significant differences at  $P < 0.05$ . a: non-irradiated nerve crushed muscle **vs.** contralateral control; b: irradiated nerve crushed muscle **vs.** contralateral control.



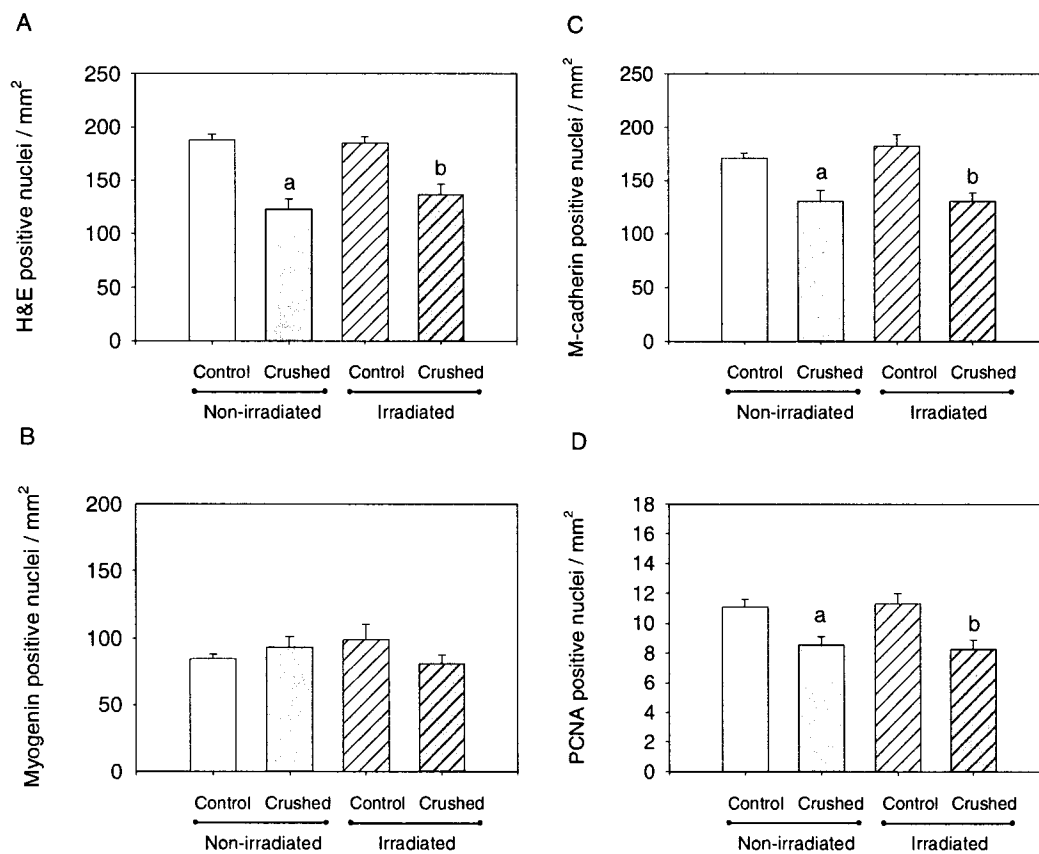


**Figure 4-6.** Positively stained myonuclei number per mm<sup>2</sup> corrected for fibre atrophy (A) H&E, (B) myogenin, (C) M-cadherin and (D) PCNA. “a” and “b” indicate significant differences at P < 0.05. a: non-irradiated nerve crushed muscle **vs.** contralateral control; b: irradiated nerve crushed muscle **vs.** contralateral control.

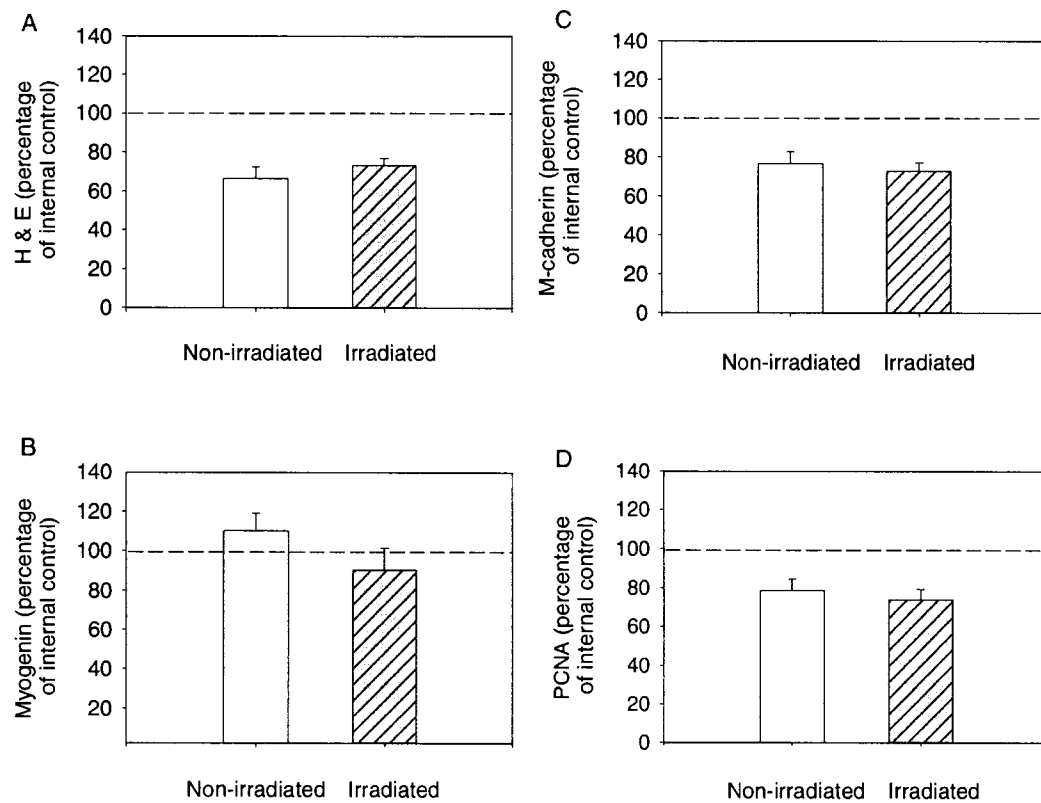


**Figure 4-7.** Changes in the positively stained myonuclei number per  $\text{mm}^2$  (corrected for fibre atrophy) of the treated *tibialis anterior* muscles relative to their respective contralateral controls. The values of contralateral controls are 100%. Data are calculated from those displayed in Figure 4-6. (A) H&E, (B) myogenin, (C) M-cadherin and (D) PCNA.

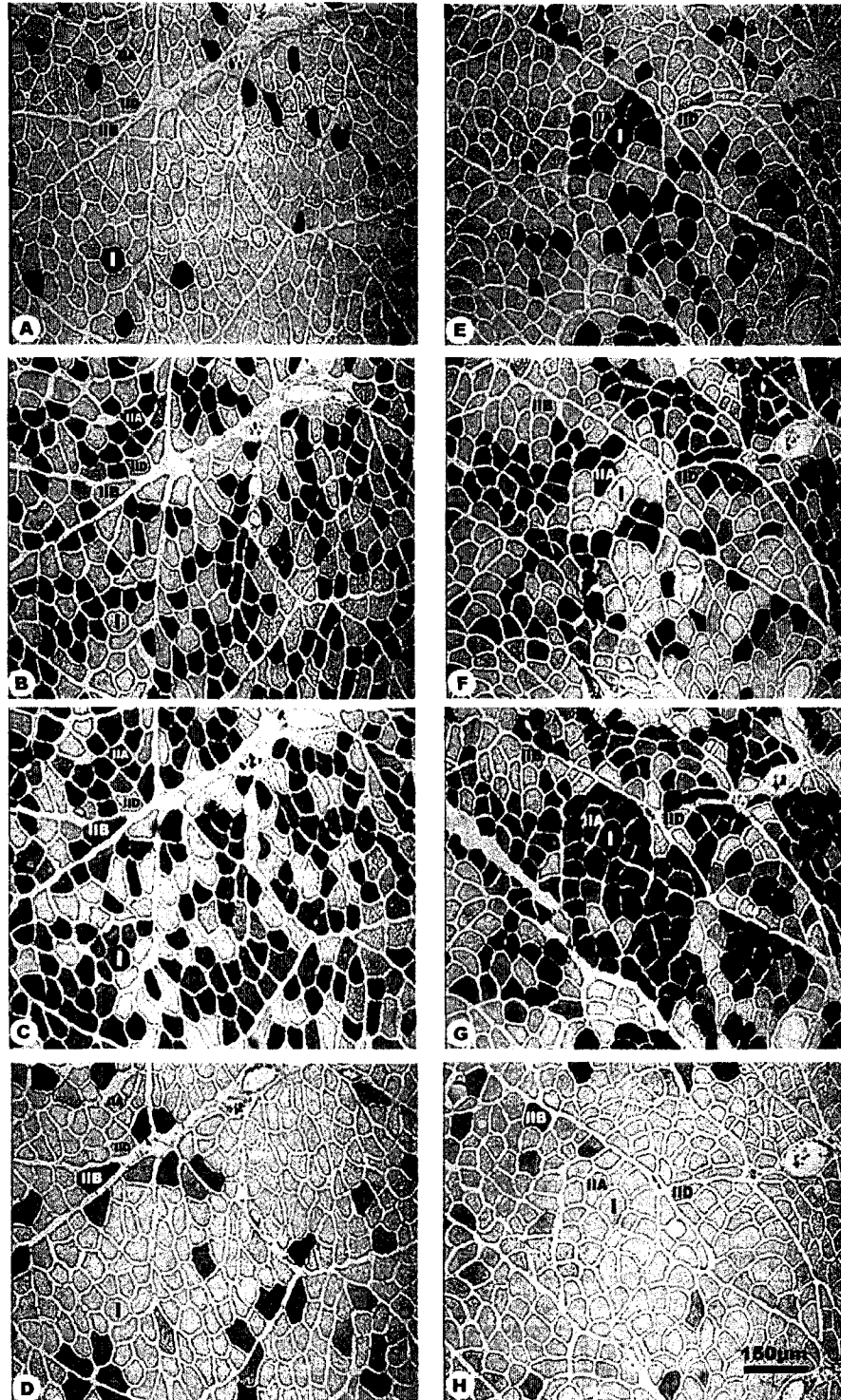


**Figure 4-8.** Representative photomicrographs of MHC immunostaining from contralateral control (A, B, C, D) and nerve crushed (E, F, G, H) *tibialis anterior* muscles. Sections are stained with: BA-D5 (type I - A, E); SC-71 (type IIA - B, F); BF-35 (invert stain of type IID(X) - C, G) and BF-F3 (type IIB - D, H).

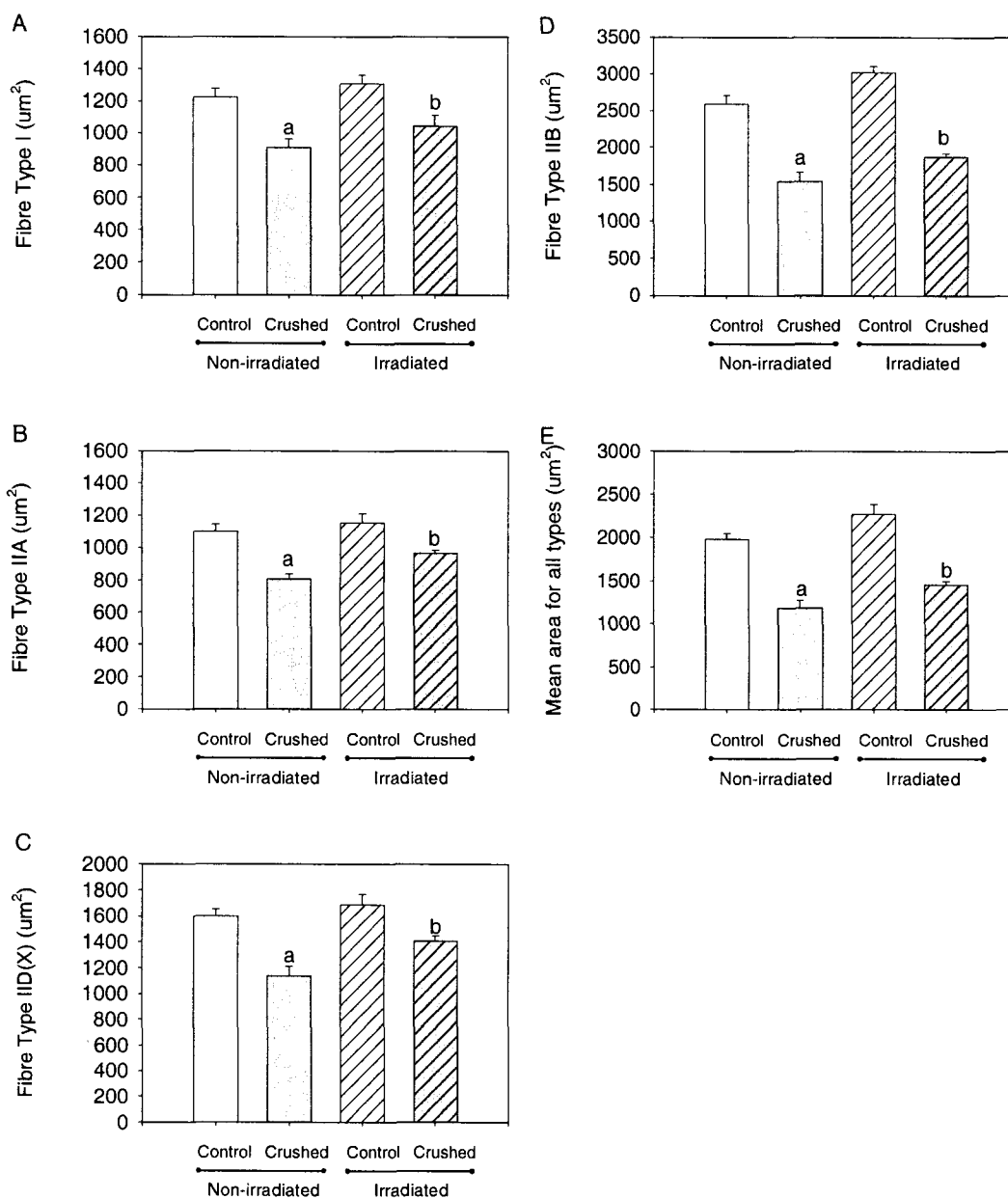


**Figure 4-9.** *Tibialis anterior* muscles fibre cross-sectional area for each fibre type and average for all fibres (hybrid fibres are counted as both types they express) “a” and “b” indicate significant differences at  $P < 0.05$ . a: non-irradiated nerve crushed muscle **vs.** contralateral control; b: irradiated nerve crushed muscle **vs.** contralateral control.

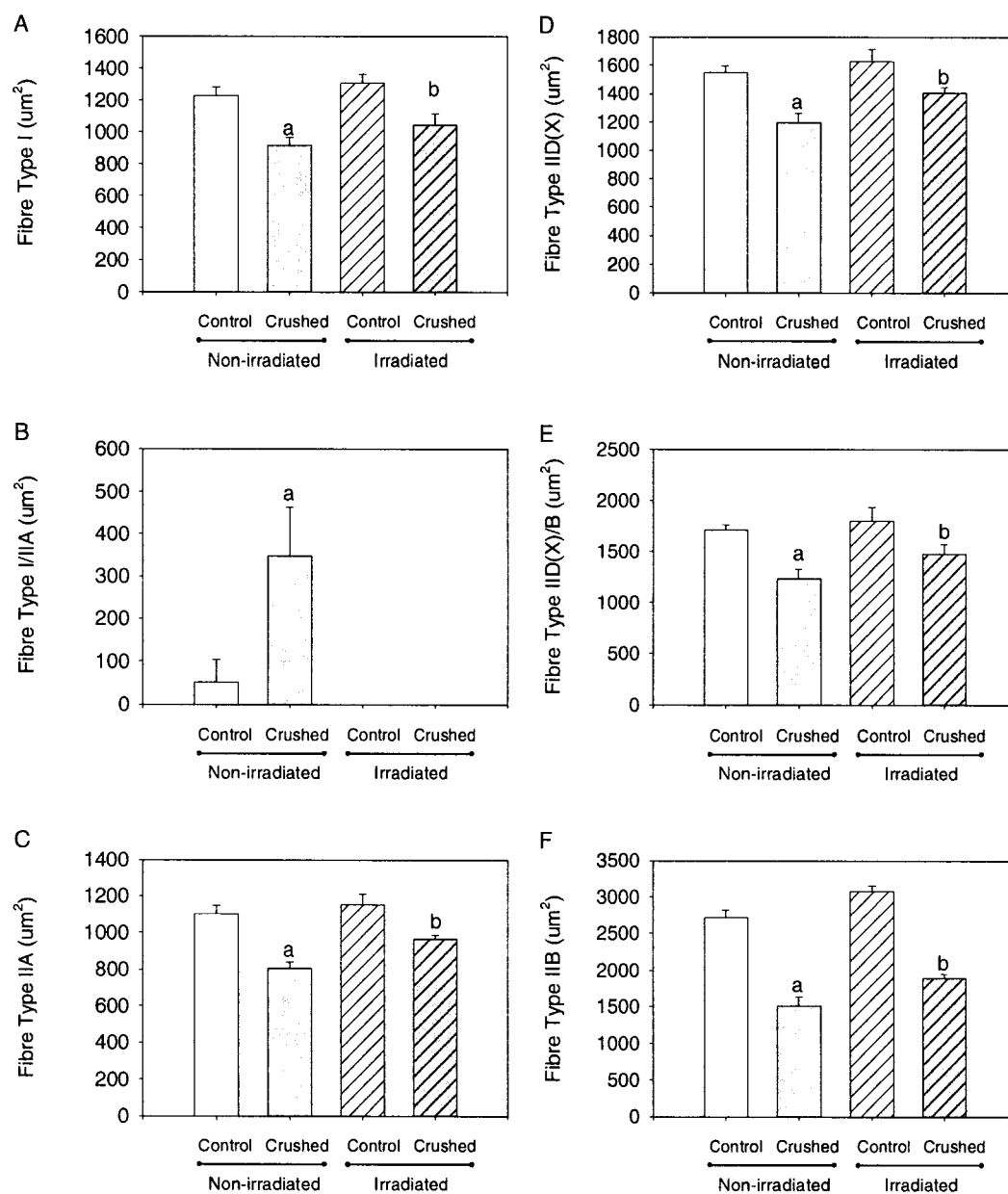


**Figure 4-10.** *Tibialis anterior* muscles fibre cross-sectional area for each fibre type (hybrid fibres are counted separately). “a” and “b” indicate significant differences at  $P < 0.05$ . a: non-irradiated nerve crushed muscle vs. contralateral control; b: irradiated nerve crushed muscle vs. contralateral control.

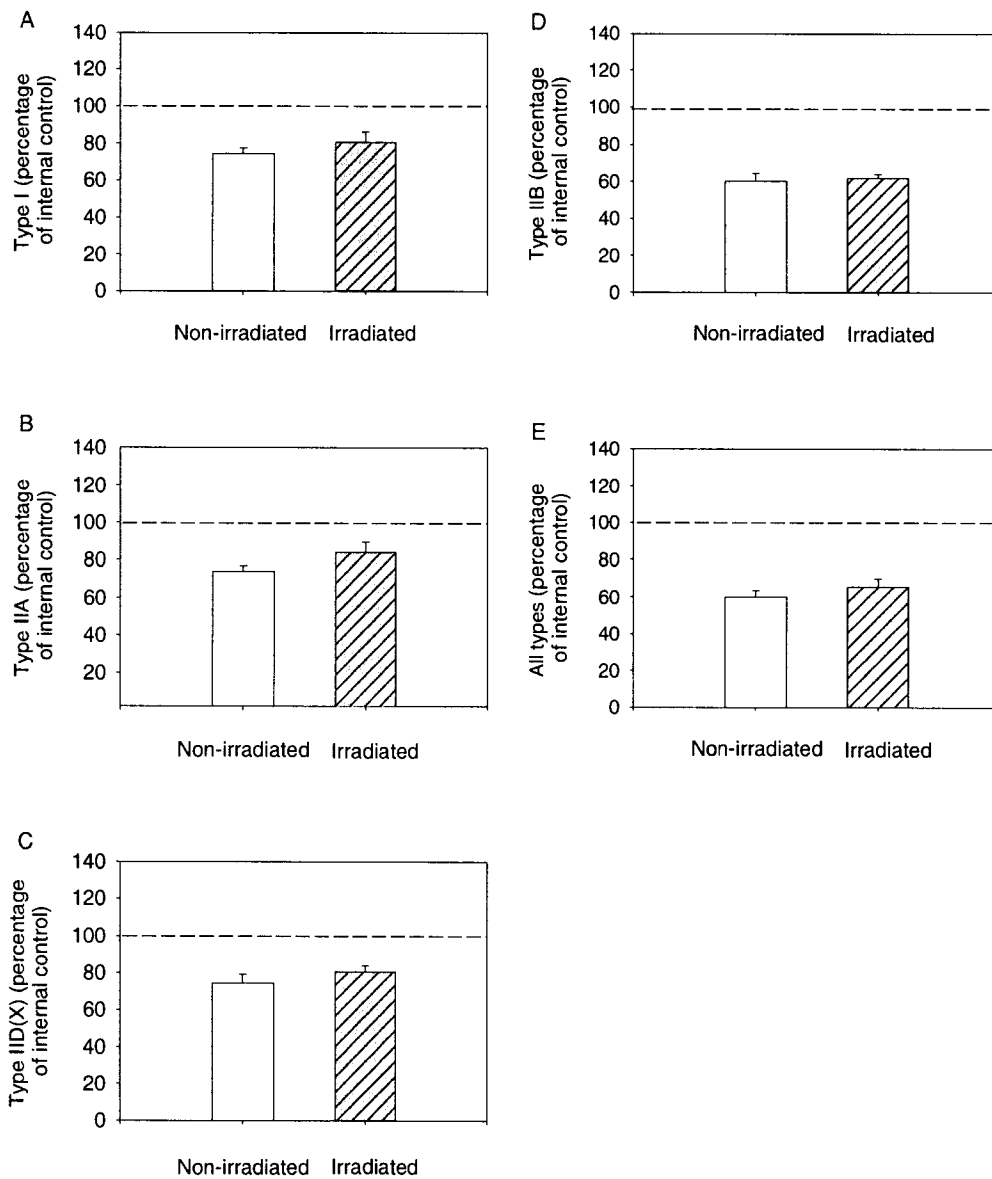


**Figure 4-11.** Changes in the muscle fibre cross-sectional areas of the treated *tibialis anterior* muscles relative to their respective contralateral controls. The values of contralateral controls are 100%. Data are calculated from those displayed in Figure 4-9.

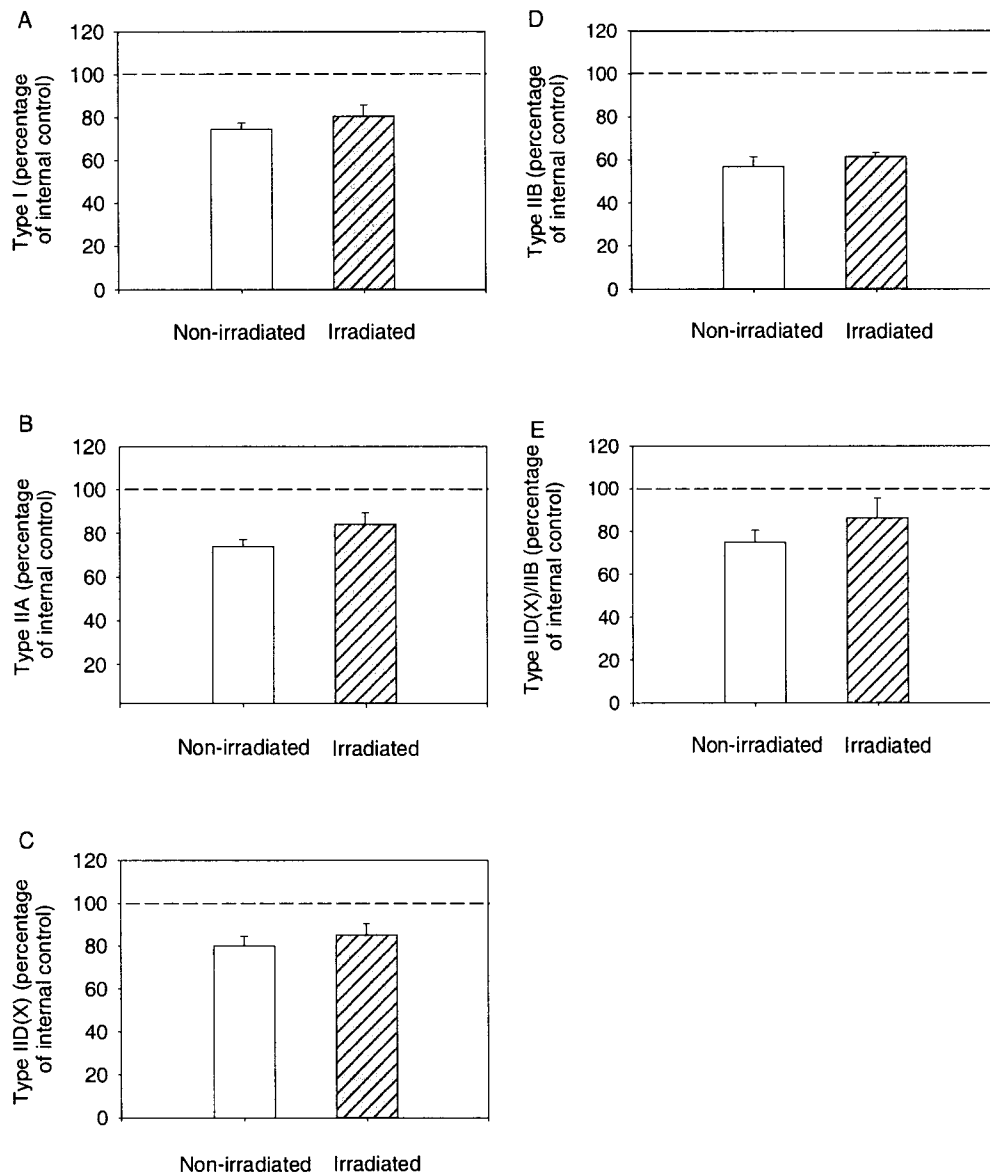


**Figure 4-12.** Changes in the muscle fibre cross-sectional area for each fibre type (hybrid fibres are counted separately) of the treated *tibialis anterior* muscles relative to their respective contralateral controls. The values of contralateral controls are 100%. Data are calculated from those displayed in Figure 4-10.

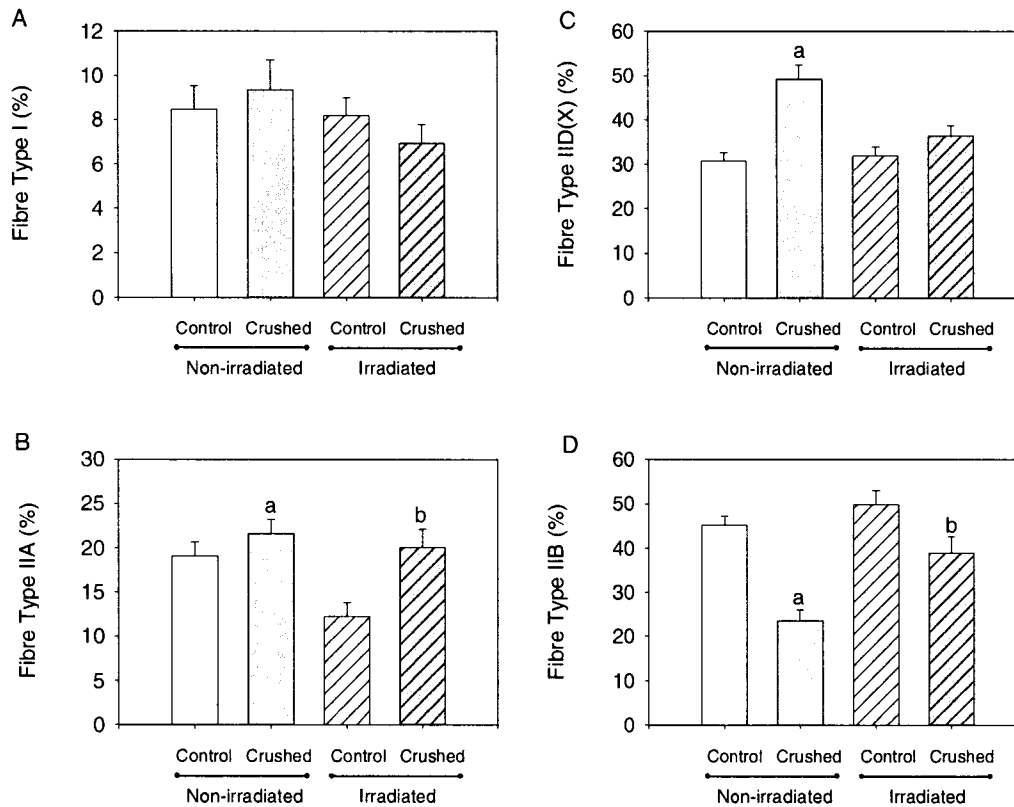


**Figure 4-13.** Fibre type percentage analyzed by immunohistochemistry (hybrid fibres are counted as both types they express). “a” and “b” indicate significant differences at  $P < 0.05$ . a: non-irradiated nerve crushed muscle **vs.** contralateral control; b: irradiated nerve crushed muscle **vs.** contralateral control.



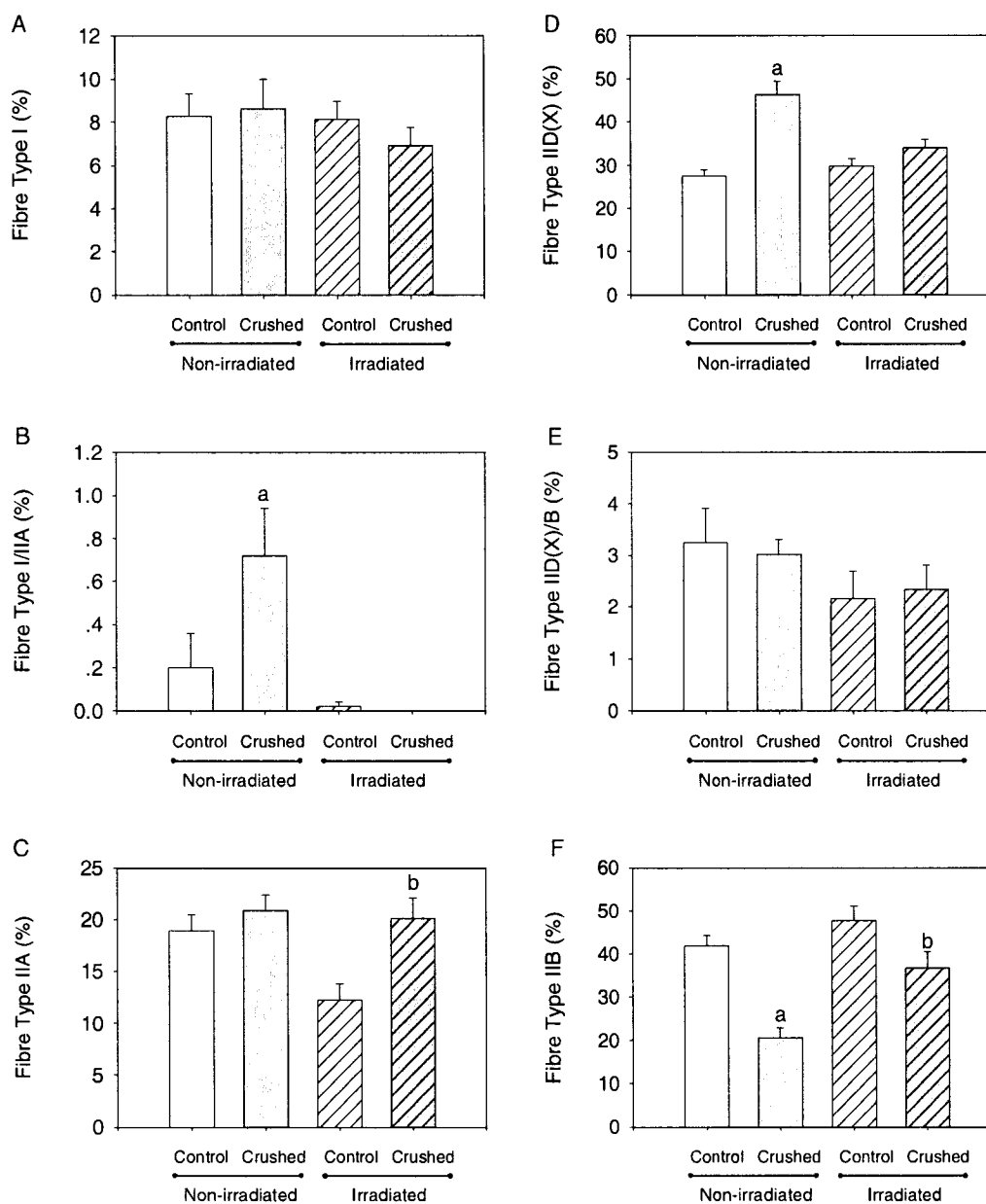


**Figure 4-14.** Fibre type percentage analyzed by immunohistochemistry (hybrid fibres are counted separately). “a” and “b” indicate significant differences at  $P < 0.05$ . a: non-irradiated nerve crushed muscle **vs.** contralateral control; b: irradiated nerve crushed muscle **vs.** contralateral control.

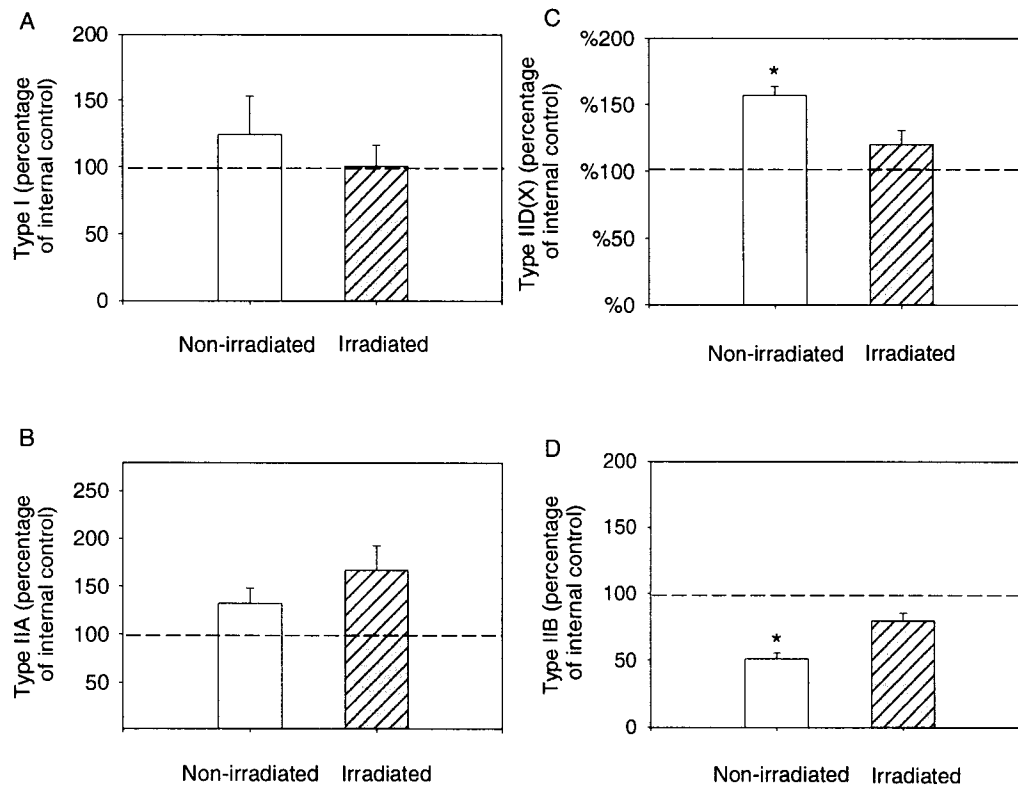


**Figure 4-15.** Changes in the fibre type percentage of the treated *tibialis anterior* muscles relative to their respective contralateral controls. The values of contralateral controls are 100%. Data are calculated from those displayed in Figure 4-13. "\*" indicates significant differences at  $P < 0.05$ .

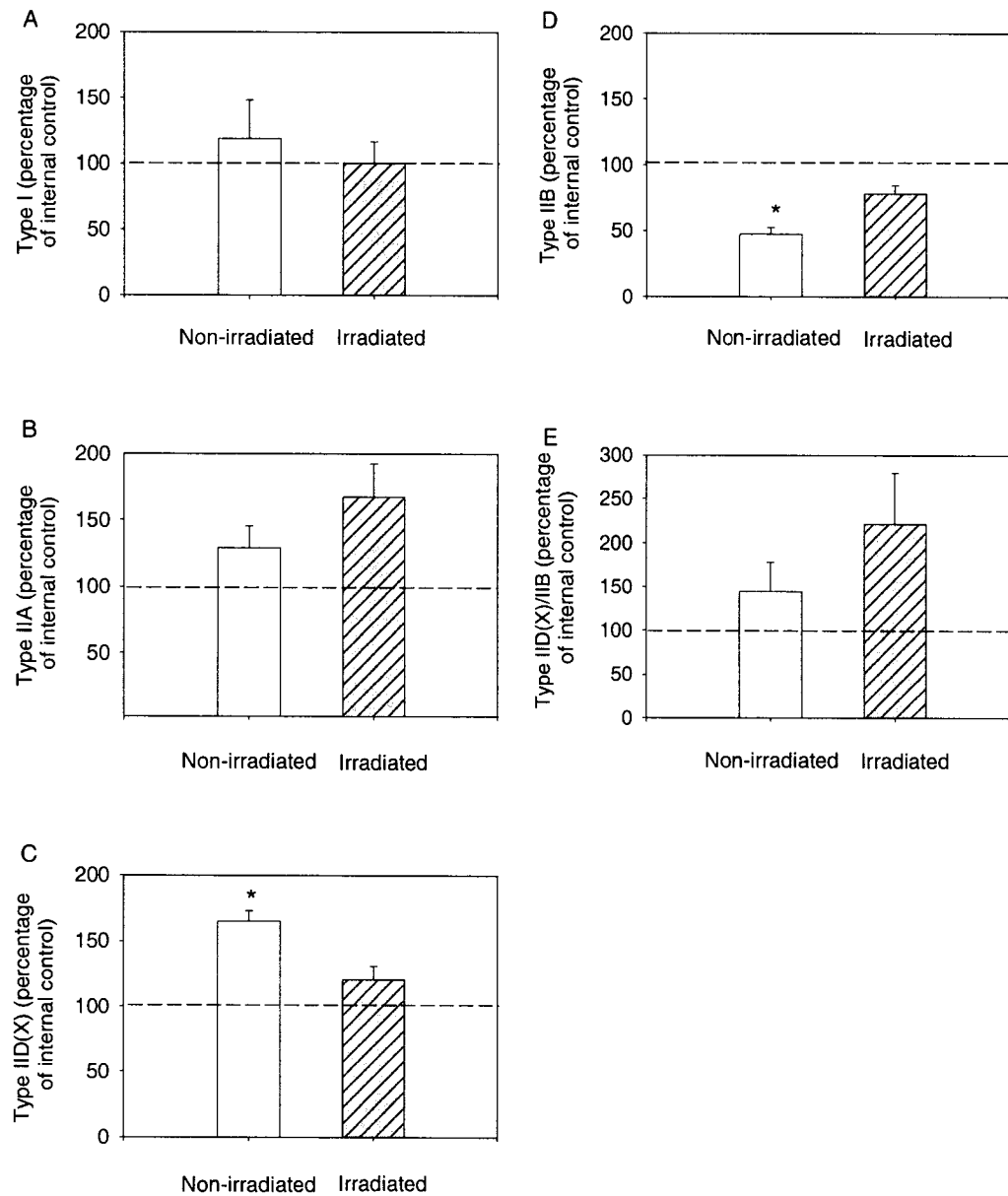


**Figure 4-16.** Changes in the fibre type percentage (hybrid fibres are counted separately) of the treated *tibialis anterior* muscles relative to their respective contralateral controls. The values of contralateral controls are 100%. Data are calculated from those displayed in Figure 4-14. “\*” indicates significant differences at  $P < 0.05$ .

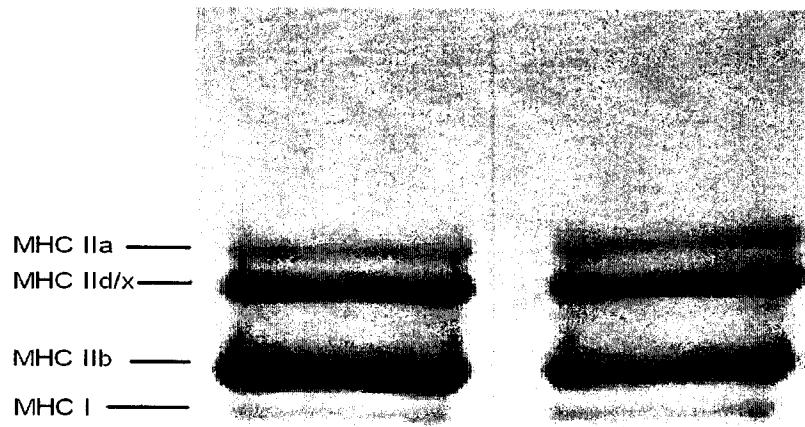


**Figure 4-17.** Representative MHC separation via SDS-PAGE.

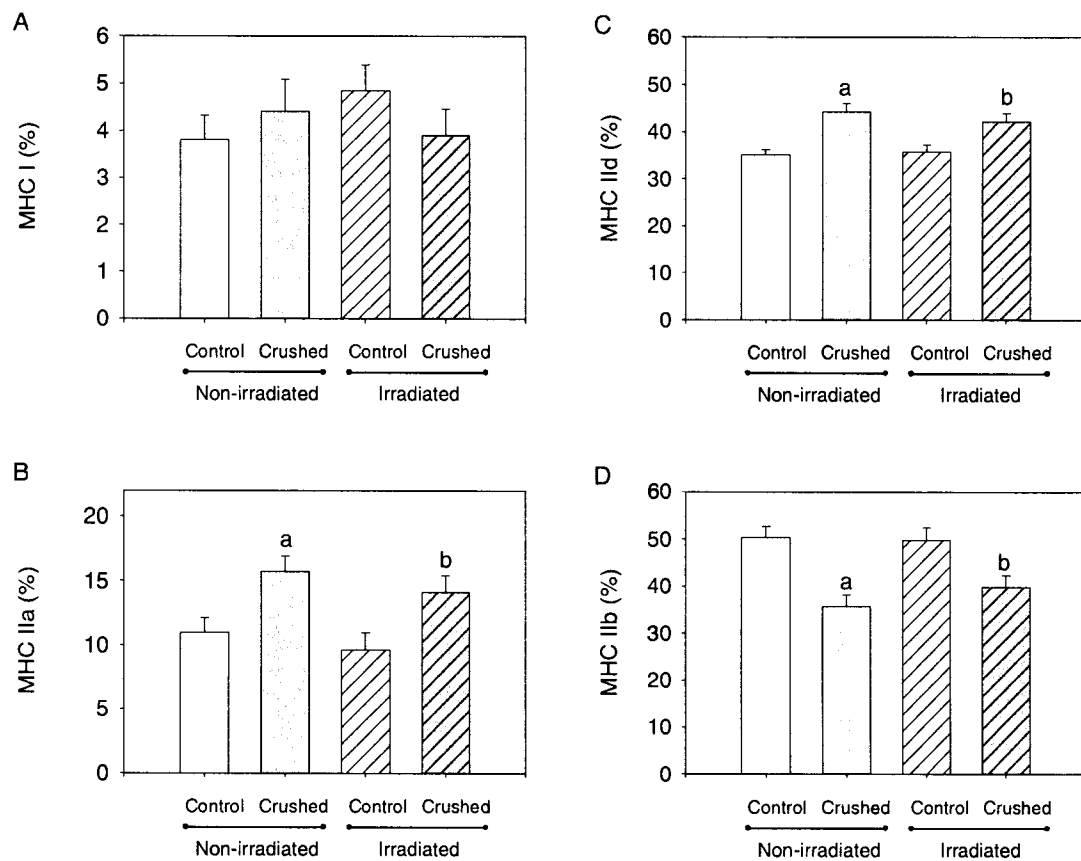


**Figure 4-18.** MHC content analyzed by SDS-PAGE. “a” and “b” indicate significant differences at  $P < 0.05$ . a: non-irradiated nerve crushed muscle *vs.* contralateral control; b: irradiated nerve crushed muscle *vs.* contralateral control.

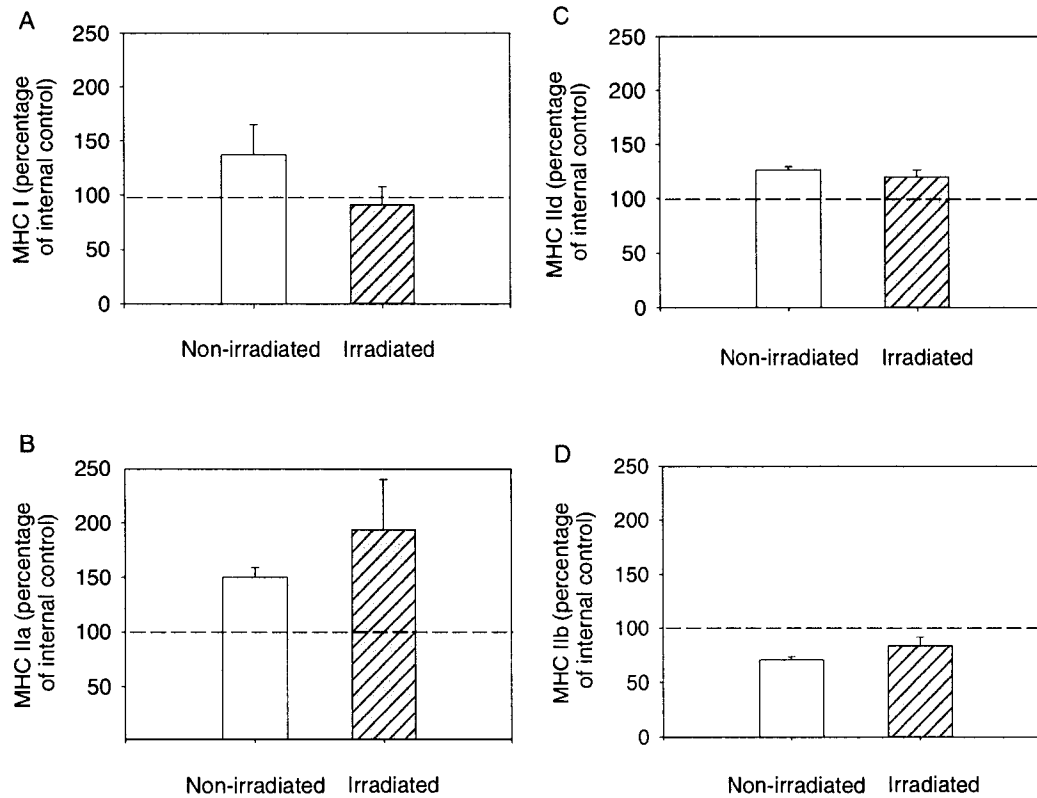


**Figure 4-19.** Changes in the MHC content of the treated *tibialis anterior* muscles relative to their respective contralateral control. The values of contralateral controls are 100%. Data are calculated from those displayed in Figure 4-18.

## CHAPTER V: DISCUSSION

### Introduction

The purpose of the present study was to investigate the mechanism involved in the recovery of atrophied skeletal muscle after prolonged denervation, and especially the role satellite cells play in this process. Based on earlier studies on muscle denervation atrophy and reinnervation recovery, we hypothesized that during twelve weeks of regeneration with reinnervation, satellite cells would help to contribute to the recovery of the reinnervated *tibialis anterior* muscle, and muscle cross-sectional area and muscle force in the treated leg would recover to those of the control leg. In contrast, we expected repeated  $\gamma$ -irradiation conducted on the treated leg to attenuate recovery due to the elimination of the satellite cell contribution to muscle repair. The main findings of the present study showed that all the treated muscles reached ~73% of their “controls” mass and ~54% of their “controls” force, respectively. Although the repeated  $\gamma$ -irradiation did not seem to affect muscle recovery, the results did suggest that the contribution of satellite cells to the repair of atrophied muscle is crucial during the phase of recovery and limitation of this cell population could be a reason for the poor recovery seen in prolonged denervation.

### Muscle Reinnervation

The repeated nerve crushes we employed in the present study was a modification of previous studies (Fu & Gordon, 1995a; Fu & Gordon, 1995b) to

induce prolonged denervation followed by self reinnervation. Reinnervation can take place by the regrowth of axons down mechanically undamaged channels following a crush that does not sever the entire nerve (Carlson, 1981). Previous studies have suggested that repeated nerve injuries in adult animals can enhance sprouting from the proximal stump and result in faster regeneration and reinnervation (McQuarrie *et al.*, 1977; McQuarrie & Grafstein, 1973). This regime also allowed us to retain the integrity of the basement membrane, associated Schwann cells, and the substrate and trophic support afforded to regenerating axons by these structures, thus eliminating potential degeneration of the basement membrane which otherwise could influence recovery from reinnervation (Fu & Gordon, 1995a; Fu & Gordon, 1995b; Carlson, 1981). As a result, the reinnervation of the *tibialis anterior* muscle was quite successful, as evidenced by motor unit size and number within the normal range (Fu & Gordon, 1995a; Fu & Gordon, 1995b; Totosy de Zepetnek *et al.*, 1992b; Totosy de Zepetnek *et al.*, 1992a) and indistinguishable NCAM staining from control muscles. Using this experimental approach, we restricted most of our analysis to the intrinsic muscle factors when studying the recovery of the reinnervated muscle after prolonged denervation. In addition, the lower but within normal range motor unit number observed in irradiation group compared with non-irradiation group indicates that the  $\gamma$ -irradiation employed in this study did not significantly impede nerve regeneration, which can be due to the 28-day period given for the nerve to grow back to the muscle after the last crush. This method did not, however, preclude possible influences from nerve branching within the



target muscle, because nerve branches may not be able to find the former endplates and restore the original innervating pattern.

### **Structural and Functional Recovery After Reinnervation**

After twelve weeks of regeneration, muscle mass reached ~73% of control values, whereas muscle force only recovered to ~54% of the controls. These values are similar to those seen in other denervation studies. Since we excluded the reinnervation deficit caused by deterioration of the basement membrane, our results suggest that the incomplete recovery seen in this study might be due to (1) an inability of muscle fibres to fully regenerate; (2) a failure to restore the branching of nerve fibres within the muscle to the original pattern, which might be critical for muscle recovery (Carlson *et al.*, 1983); (3) the twelve weeks of regeneration not being long enough to allow full recovery (Jakubiec-Puka *et al.*, 1990); or (4) a combination of some, or all, of the above. A previous study suggested that a critical factor for a successful muscle graft is integrated nerve paths within the muscle, since the regenerating nerve can follow these paths to find the original motor endplates (Carlson *et al.*, 1983): these authors showed that nerve-intact muscle grafts fully restored their mass, even after delayed reinnervation (Carlson *et al.*, 1983). Thus, in addition to the degeneration of the basement membrane suggested by Fu and Gordon (1995), the deterioration of nerve pathways within the muscle is also a possible cause for poor recovery in long-term denervated muscle.

Muscle restoration after denervation results from an increase in cytoplasmic volume and additional myonuclei, which in turn restores muscle mass and force. Since myonuclei do not possess the ability to replicate, the additional myonuclei needed for muscle repair are dependent on satellite cells. It was, therefore, surprising to see that the mass and force of the irradiated muscles recovered to the same extent as the non-irradiated muscles, since  $\gamma$ -irradiation was postulated to attenuate muscle repair by sterilizing the satellite cell population. One explanation could be that the frequency of  $\gamma$ -irradiation was not high enough and that as a result some satellite cells survived the  $\gamma$ -irradiation through DNA repair and mitotic recovery (Mozdziak *et al.*, 1996). Our data suggest that a more likely explanation is that satellite cell contribution was mostly achieved prior to  $\gamma$ -irradiation. This possibility will be addressed in detail later.

Muscle fibre cross-sectional area was reduced in all treated muscles, although to different levels with regard to different fibre types. The largest decrease (only ~60% of control) was associated with type-IIB fibres, and could be explained by transitions from type-IIB to other fibre types. Although fibre type transition also occurred within the type-IIA and -IID(X), the increased proportions of these two fibre types were not sufficient to induce any discernable changes in their cross-sectional area. Thus the ratio of treated to control muscle fibre cross-sectional area was consistent for type-I, -IIA and IID(X) (~75%) within the non-irradiated or irradiated groups. The similar recovery ratio in irradiated compared with non-irradiated muscles was in line with our mass and force recovery results in the sense that  $\gamma$ -irradiation did not impede muscle recovery from denervation.

Except for muscle force production, the functional properties of recovered muscles did not exhibit much change. The small but significant decreases in TTP and 1/2RT seen in the irradiated muscles indicate that this group had a faster contraction speed. The motor unit size and number seen in the non-irradiated and irradiated *tibialis anterior* were within normal range (Fu & Gordon, 1995a; Fu & Gordon, 1995b; Totosy de Zepetnek *et al.*, 1992b; Totosy de Zepetnek *et al.*, 1992a), indicating that functional connections between regenerating motor axons and the target muscle fibres were successful. However, the motor unit number in the irradiated muscle was lower than that in the non-irradiated muscle, which could be due to that the irradiation impeded the reinnervation. Without testing the contralateral control leg, however, we could not conclude that irradiation changed the pattern of reinnervation because motor unit number varies individually within a range. Since whole muscle force recovery of irradiated was no less than that seen in non-irradiated muscles, a compensatory enlarged motor unit size was postulated. This was indicated by the larger motor unit size measured in the irradiated muscle. In summary, these functional data suggest that the repeated nerve crush model was effective for inducing long-term denervation. Compared with the case when sectioned nerve stumps were sutured after prolonged denervation, self-reinnervation following repeated nerve crush resulted in a much better recovery (Fu & Gordon, 1995a; Fu & Gordon, 1995b).

### **Muscle Fibre Type Transition**

After repeated denervation followed by reinnervation, the *tibialis anterior* muscle had an altered fibre type distribution, which is a result of transitions from type-IIB to types –IID(X) and –IIA, whereas type-I fibre proportion did not change significantly. These transitions were shown by immunohistochemistry and also confirmed by SDS-PAGE. The results agree well with claims made from previous studies that denervation could induce fast-to-slow fibre type transformation in fast muscles (Schiaffino *et al.*, 1988; Carraro *et al.*, 1985; Jakubiec-Puka *et al.*, 1990). It has also been reported that during fast-to-slow fibre type transitions, satellite cells preferentially fused to type-IIB fibres, increasing myonuclear content, followed by the appearance of MHCIIa within these fibres (Putman *et al.*, 2000). It was further suggested by these authors that the increase in muscle nuclei of the fast fibres might be a prerequisite for fast-to-slow fibre type transitions. Thus, satellite cell fusion to fast fibres seems to be a critical step before fibre type transition. Available results from the present study do not conflict with this hypothesis, as a higher type IIB, lower typeIID(x) and an absence of hybrid typeI/IIA fibres in contrast with the non-irradiated muscle, indicate an attenuated transition in the irradiated muscle. However, fibre type transition did occur in the irradiated muscle, although to a lesser extent. This could be the result of some transitions induced by denervation before the muscles were irradiated, and/or some transformations without satellite cells being involved. Rosenblatt *et al.* (1992, 1993, 1994) reported that satellite cell sterilization by 25-Gy  $\gamma$ -irradiation did not prevent fast-to-slow fibre type

transitions and concluded that satellite cell involvement was not a requirement for fibre type transitions. However, a single dose of 25-Gy  $\gamma$ -irradiation used in those studies was shown to be insufficient to permanently block satellite cell activity. In this regard, Martins *et al.* (2005) employed repeated exposure to 25-Gy of  $\gamma$ -irradiation to ensure sterilization of the satellite cell population. Despite complete satellite cell sterilization, Martins *et al.* (2005) found that fibre type transitions were attenuated but not completely abolished in the absence of a viable population of satellite cells. Collectively, satellite cells appear to play a role in fibre type transition induced by denervation, and myonuclei also have considerable adaptive potential during the process.

### **Satellite Cell Involvement**

Satellite cells were involved in the repair of the atrophied muscle as evidenced by the decrease of total myonuclei and unchanged myogenin-positive nuclei in the treated muscles because these data indicate that satellite cells in the differentiation and fusion phase were in the process of restoring the decreased myonuclei number. Following denervation, satellite cells were reported to be activated during the first two to three weeks and some were able to fuse directly with differentiated muscle fibres (Borisov *et al.*, 2005). However, these satellite cells failed to terminally differentiate without innervation and the reason remains unclear. In the present study, the repeated nerve crush injury was expected to provoke several waves of satellite cell proliferation by denervating the *tibialis anterior* muscle every time the muscle started to be reinnervated. It was reported that at 2 months of denervation, satellite cell

content in the denervated muscle reached the highest levels (Viguie *et al.*, 1997). This time point is close to the time frame (70 days) of the present study when the *tibialis anterior* started receiving innervation after the final nerve crush. The expectation was that the progeny produced by satellite cell proliferation contribute to the restoration of myonuclei loss during denervation, by fusing with muscle fibres. This was confirmed by the myogenin staining; after twelve weeks of recovery, satellite cells in their late phase of differentiation and fusion were still present at higher level, as a result of earlier satellite cell progeny going through the final differentiation step. Since the  $\gamma$ -irradiation was not conducted before the 70th day, satellite cells from both non-irradiated and irradiated groups were perhaps able to proliferate to the same extent. This might explain the similar number of myogenin-positive nuclei seen in the irradiated muscle, since they could be the result of earlier satellite cell proliferation-differentiation before  $\gamma$ -irradiation was conducted.

As mentioned earlier, it was surprising to see that the recovery of muscle mass, force, and cross-sectional area in the irradiated group reached similar levels to that of the non-irradiated group. It was expected that by using  $\gamma$ -irradiation to block the contribution of satellite cells to muscle regeneration, irradiated muscles would not recover to the same degree. However, the nuclear staining results suggested no difference between irradiated and non-irradiated muscles, which might shed light on the time course that is critical for muscle recovery after denervation followed by reinnervation. Since satellite cells can be activated as early as the first two to three weeks of denervation and since some

are even able to fuse directly with differentiated muscle fibres (Borisov *et al.*, 2005), it might be possible that the greatest extent of recovery had already started during the ~70 days of denervation in the present study, and that the progeny produced by satellite cell proliferation were already sufficient for muscle repair. All that these progeny needed in order to facilitate terminal differentiation was reinnervation, which commenced at this time. Thus, although the subsequent  $\gamma$ -irradiation blocked satellite cells from further proliferation, it apparently did not impede muscle recovery that utilized satellite cell progeny that were already present. Another possibility is that satellite cells possess such a huge capacity for self renewal and repair that even after  $\gamma$ -irradiation, there were still numerous cells survived and contributed to muscle recovery. Available results from PCNA staining suggest that a 30 Gy  $\gamma$ -irradiation was not enough to maintain sterilization of the satellite cell pool for four weeks. With the findings that total myonuclei, quiescent satellite cells and the proliferating cells all decreased to similar levels in the treated muscles, which indicate that satellite cell number decreased significantly during denervation and recovery, one can conclude that the poor recovery ability of skeletal muscle after prolonged denervation is partially due to a limited satellite cell pool.

### **Future Research Directions**

The present study tried to focus on intrinsic muscle factors contributing to poor muscle recovery after prolonged denervation. Although a more often use of  $\gamma$ -irradiation right after each nerve crushing could ensure a depletion of satellite cells, letting us compare muscle recovery with or without the contribution of

satellite cells, it could also affect the nerve regeneration. Thus, the experimental design we employed seems not to be an optimal model to address this subject. Approaches that can block satellite cell activity without affecting nerve regeneration would be more helpful.

Muscle stem cell transplantation for therapeutic purposes has received a lot of attention recently (Torrente *et al.*, 2003; Torrente *et al.*, 2000; El Fahime *et al.*, 2000; Partridge, 2003), but the results to date have been far from satisfactory. It has been suggested that a sub-population of satellite cells that function as stem cells are more potent in cell transplantation, in contrast to those that are simply available for fusion (Morgan & Partridge, 2003). The present study suggest that a limited satellite cell pool might underlie some of the incomplete recovery of skeletal muscle structure and function after a period of prolonged denervation, thus manipulation of this cell population appears to be a promising approach for improving recovery. However, it is still critical to fundamentally understand the behavior of these satellite cells before successful cell therapy can be achieved.

Although it is well recognized that satellite cell regulation occurs in response to a number of potential growth factors that arise from a number of sources it remains obscure which of these factors are effective *in vivo*. Most studies to date, used *in vitro* experiments and thus excluded possible interactions between factors. More investigations are also needed to understand whether satellite cells are regulated by local signals secreted from adjacent fibres and tissues, or by circulating systemic factors. Furthermore, cell lineage specific markers, or more advanced techniques to identify satellite cells *in vivo*, will be helpful in order



to study this group of cells more thoroughly, and especially their role in myofibre phenotype determination.

### **Conclusion**

Successful muscle structural and functional recovery after delayed nerve repair or injuries is rarely seen, and the reason is not well understood. Denervation causes fundamental changes in the motor control system, and it is likely that a complex system governs the process of recovery. Research continues to support the notion that successful regeneration of the motor nerve plays a crucial role in the process. At the same time, it has also been recognized that intrinsic muscle factors are essential, although it is not clear to what extent they contribute to incomplete recovery.

Nevertheless, the findings of the present study add to the body of knowledge concerning satellite cells, suggesting that during muscle recovery after denervation followed by reinnervation, satellite cells are actively involved by proliferating and fusing to atrophied muscle fibres. Skeletal muscle recovery after prolonged denervation depends on complete reinnervation of the muscle and successful differentiation of satellite cells. A limited satellite cell pool might be partially responsible for the poor recovery ability of skeletal muscle after prolonged denervation. Satellite cells also appear to play some role in fibre type transformation during denervation, suggesting their involvement in muscle phenotype determination.

## CHAPTER VI: LIST OF REFERENCES

Anastasi, S., Giordano, S., Sthandier, O., Gambarotta, G., Maione, R., Comoglio, P., & Amati, P. (1997). A natural hepatocyte growth factor/scatter factor autocrine loop in myoblast cells and the effect of the constitutive Met kinase activation on myogenic differentiation. *J Cell Biol.* **137**, 1057-1068.

Andermarcher, E., Surani, M. A., & Gherardi, E. (1996). Co-expression of the HGF/SF and c-met genes during early mouse embryogenesis precedes reciprocal expression in adjacent tissues during organogenesis. *Dev.Genet.* **18**, 254-266.

Baroffio, A., Hamann, M., Bernheim, L., Bochaton-Piallat, M. L., Gabbiani, G., & Bader, C. R. (1996). Identification of self-renewing myoblasts in the progeny of single human muscle satellite cells. *Differentiation* **60**, 47-57.

Bennett, M. R., McLachlan, E. M., & Taylor, R. S. (1973). The formation of synapses in reinnervated mammalian striated muscle. *J Physiol* **233**, 481-500.

Beauchamp, J. R., Morgan, J. E., Pagel, C. N., & Partridge, T. A. (1999). Dynamics of myoblast transplantation reveal a discrete minority of precursors with stem cell-like properties as the myogenic source. *J Cell Biol.* **144**, 1113-1122.

Bladt, F., Riethmacher, D., Isenmann, S., Aguzzi, A., & Birchmeier, C. (1995). Essential role for the c-met receptor in the migration of myogenic precursor cells into the limb bud. *Nature* **376**, 768-771.

Booth, F. W., Weeden, S. H., & Tseng, B. S. (1994). Effect of aging on human skeletal muscle and motor function. *Med.Sci.Sports Exerc.* **26**, 556-560.

Borisov, A. B., Dedkov, E. I., & Carlson, B. M. (2001). Interrelations of myogenic response, progressive atrophy of muscle fibers, and cell death in denervated skeletal muscle. *Anat.Rec.* **264**, 203-218.

Borisov, A. B., Dedkov, E. I., & Carlson, B. M. (2005). Abortive myogenesis in denervated skeletal muscle: differentiative properties of satellite cells, their migration, and block of terminal differentiation. *Anat.Embryol.(Berl)* **209**, 269-279.

Bornemann, A., Maier, F., & Kuschel, R. (1999). Satellite cells as players and targets in normal and diseased muscle. *Neuropediatrics* **30**, 167-175.

Bradford, M. M. (1976). A rapid and sensitive method for the quantitation of microgram quantities of protein utilizing the principle of protein-dye binding. *Anal.Biochem.* **72**, 248-254.

Bravo, R., Frank, R., Blundell, P. A., & Macdonald-Bravo, H. (1987). Cyclin/PCNA is the auxiliary protein of DNA polymerase-delta. *Nature* **326**, 515-517.

Bridge, P. M., Ball, D. J., Mackinnon, S. E., Nakao, Y., Brandt, K., Hunter, D. A., & Hertl, C. (1994). Nerve crush injuries--a model for axonotmesis. *Exp.Neurol.* **127**, 284-290.

Carlson, B. M. (1981). Denervation, reinnervation, and regeneration of skeletal muscle. *Otolaryngol.Head Neck Surg.* **89** , 192-196.

Carlson, B. M., Dedkov, E. I., Borisov, A. B., & Faulkner, J. A. (2001). Skeletal muscle regeneration in very old rats. *J Gerontol.A Biol.Sci.Med.Sci.* **56**, B224-B233.

Carlson, B. M. & Faulkner, J. A. (1989). Muscle transplantation between young and old rats: age of host determines recovery. *Am J Physiol* **256**, C1262-C1266.

Carlson, B. M., Foster, A. H., Bader, D. M., Hnik, P., & Vejsada, R. (1983). Restoration of full mass in nerve-intact muscle grafts after delayed reinnervation. *Experientia* **39**, 171-172.

Carraro, U., Morale, D., Mussini, I., Lucke, S., Cantini, M., Betto, R., Catani, C., Dalla, L. L., Danieli, B. D., & Noventa, D. (1985). Chronic denervation of rat hemidiaphragm: maintenance of fiber heterogeneity with associated increasing uniformity of myosin isoforms. *J Cell Biol.* **100**, 161-174.

Chakravarthy, M. V., Davis, B. S., & Booth, F. W. (2000). IGF-I restores satellite cell proliferative potential in immobilized old skeletal muscle. *J of Applied Physiol* **89**, 1365-1379.

Cornelison, D. D. & Wold, B. J. (1997). Single-cell analysis of regulatory gene expression in quiescent and activated mouse skeletal muscle satellite cells. *Dev.Biol.* **191**, 270-283.

Covault, J. & Sanes, J. R. (1986). Distribution of N-CAM in synaptic and extrasynaptic portions of developing and adult skeletal muscle. *J Cell Biol.* **102**, 716-730.

Darr, K. C. & Schultz, E. (1987). Exercise-induced satellite cell activation in growing and mature skeletal muscle. *J of Applied Physiol* **63**, 1816-1821.

Dedkov, E. I., Borisov, A. B., & Carlson, B. M. (2003a). Dynamics of postdenervation atrophy of young and old skeletal muscles: differential responses of fiber types and muscle types. *J Gerontol.A Biol.Sci.Med.Sci.* **58**, 984-991.

Dedkov, E. I., Borisov, A. B., Wernig, A., & Carlson, B. M. (2003b). Aging of skeletal muscle does not affect the response of satellite cells to denervation. *J Histochem.Cytochem.* **51**, 853-863.

Dedkov, E. I., Kostrominova, T. Y., Borisov, A. B., & Carlson, B. M. (2001). Reparative myogenesis in long-term denervated skeletal muscles of adult rats results in a reduction of the satellite cell population. *Anat.Rec.* **263**, 139-154.

Di Donna, S., Renault, V., Forestier, C., Piron-Hamelin, G., Thiesson, D., Cooper, R. N., Ponsot, E., Decary, S., Amouri, R., Hentati, F., Butler-Browne, G. S., & Mouly, V. (2000). Regenerative capacity of human satellite cells: the mitotic clock in cell transplantation. *Neurol.Sci.* **21**, S943-S951.

El Fahime, E., Torrente, Y., Caron, N. J., Bresolin, M. D., & Tremblay, J. P. (2000). In vivo migration of transplanted myoblasts requires matrix metalloproteinase activity. *Exp.Cell Res.* **258**, 279-287.

Floss, T., Arnold, H. H., & Braun, T. (1997). A role for FGF-6 in skeletal muscle regeneration. *Genes Dev.* **11**, 2040-2051.

Fu, S. Y. & Gordon, T. (1995a). Contributing factors to poor functional recovery after delayed nerve repair: prolonged denervation. *J Neurosci.* **15**, 3886-3895.

Fu, S. Y. & Gordon, T. (1995b). Contributing factors to poor functional recovery after delayed nerve repair: prolonged axotomy. *J Neurosci.* **15**, 3876-3885.

Gibson, M. C. & Schultz, E. (1982). The distribution of satellite cells and their relationship to specific fiber types in soleus and extensor digitorum longus muscles. *Anat.Rec.* **202**, 329-337.

Gillies, N. E. (1987). Effects of radiations on cells. *Br.Med.J (Clin.Res.Ed)* **295**, 1390-1391.

Gordon, T. & Stein, R. B. (1985). Temperature effects on the kinetics of force generation in normal and dystrophic mouse muscles. *Exp.Neurol.* **89**, 348-360.

Hamalainen, N. & Pette, D. (1996). Slow-to-fast transitions in myosin expression of rat soleus muscle by phasic high-frequency stimulation. *FEBS Lett.* **399**, 220-222.

Hansen, G., Martinuk, K. J., Bell, G. J., MacLean, I. M., Martin, T. P., & Putman, C. T. (2004). Effects of spaceflight on myosin heavy-chain content, fibre morphology and succinate dehydrogenase activity in rat diaphragm. *Pflugers Arch.* **448**, 239-247.

Haugk, K. L., Roeder, R. A., Garber, M. J., & Schelling, G. T. (1995). Regulation of muscle cell proliferation by extracts from crushed muscle. *J Anim Sci.* **73**, 1972-1981.

Hawke, T. J. & Garry, D. J. (2001). Myogenic satellite cells: physiology to molecular biology. *J of Applied Physiol* **91**, 534-551.

Hill, M. & Goldspink, G. (2003). Expression and splicing of the insulin-like growth factor gene in rodent muscle is associated with muscle satellite (stem) cell activation following local tissue damage. *J Physiol* **549**, 409-418.

Ijkema-Paassen, J., Meek, M. F., & Gramsbergen, A. (2002). Reinnervation of muscles after transection of the sciatic nerve in adult rats. *Muscle Nerve* **25**, 891-897.

Irintchev, A., Draguhn, A., & Wernig, A. (1990). Reinnervation and recovery of mouse soleus muscle after long-term denervation. *Neuroscience* **39**, 231-243.

- Irintchev, A., Langer, M., Zweyer, M., Theisen, R., & Wernig, A. (1997). Functional improvement of damaged adult mouse muscle by implantation of primary myoblasts. *J Physiol* **500** ( Pt 3), 775-785.
- Irintchev, A., Zeschnigk, M., Starzinski-Powitz, A., & Wernig, A. (1994). Expression pattern of M-cadherin in normal, denervated, and regenerating mouse muscles. *Dev.Dyn.* **199**, 326-337.
- Ishihara, A. & Araki, H. (1988). Effects of age on the number and histochemical properties of muscle fibers and motoneurons in the rat extensor digitorum longus muscle. *Mech.Ageing Dev.* **45**, 213-221.
- Jakubiec-Puka, A., Kordowska, J., Catani, C., & Carraro, U. (1990). Myosin heavy chain isoform composition in striated muscle after denervation and self-reinnervation. *Eur.J Biochem.* **193**, 623-628.
- Jejurikar, S. S., Marcelo, C. L., & Kuzon, W. M., Jr. (2002). Skeletal muscle denervation increases satellite cell susceptibility to apoptosis. *Plast.Reconstr.Surg.* **110**, 160-168.
- Jesse, T. L., LaChance, R., Iademarco, M. F., & Dean, D. C. (1998). Interferon regulatory factor-2 is a transcriptional activator in muscle where it regulates expression of vascular cell adhesion molecule-1. *J Cell Biol.* **140**, 1265-1276.
- Johnson, S. E. & Allen, R. E. (1993). Proliferating cell nuclear antigen (PCNA) is expressed in activated rat skeletal muscle satellite cells. *J Cell Physiol* **154**, 39-43.
- Kadhiresan, V. A., Hassett, C. A., & Faulkner, J. A. (1996). Properties of single motor units in medial gastrocnemius muscles of adult and old rats. *J Physiol* **493** ( Pt 2), 543-552.
- Kaufmann, U., Martin, B., Link, D., Witt, K., Zeitler, R., Reinhard, S., & Starzinski-Powitz, A. (1999). M-cadherin and its sisters in development of striated muscle. *Cell Tissue Res.* **296**, 191-198.
- Kuschel, R., Yablonka-Reuveni, Z., & Bornemann, A. (1999). Satellite cells on isolated myofibers from normal and denervated adult rat muscle. *J Histochem.Cytochem.* **47**, 1375-1384.

- Larsson, L. & Ansved, T. (1995). Effects of ageing on the motor unit. *Prog.Neurobiol.* **45**, 397-458.
- Lawson-Smith, M. J. & McGeachie, J. K. (1998). The identification of myogenic cells in skeletal muscle, with emphasis on the use of tritiated thymidine autoradiography and desmin antibodies. *J Anat.* **192 ( Pt 2)**, 161-171.
- Lazarides, E. & Hubbard, B. D. (1976). Immunological characterization of the subunit of the 100 A filaments from muscle cells. *Proc.Natl.Acad.Sci.U.S.A* **73**, 4344-4348.
- Lazerges, C., Daussin, P. A., Coulet, B., Boubaker, e. A., Micallef, J. P., Chammas, M., Reyne, Y., & Bacou, F. (2004). Transplantation of primary satellite cells improves properties of reinnervated skeletal muscles. *Muscle Nerve* **29**, 218-226.
- Lewis, D. M. (1972). The effect of denervation on the mechanical and electrical responses of fast and slow mammalian twitch muscle. *J Physiol* **222**, 51-75.
- Lewis, R. B. (1954). Changes in striated muscle following single intense doses of x-rays. *Lab Invest* **3**, 48-55.
- Lu, D. X., Huang, S. K., & Carlson, B. M. (1997). Electron microscopic study of long-term denervated rat skeletal muscle. *Anat.Rec.* **248**, 355-365.
- Lundblad, V. & Wright, W. E. (1996). Telomeres and telomerase: a simple picture becomes complex. *Cell* **87**, 369-375.
- Maina, F., Casagrande, F., Audero, E., Simeone, A., Comoglio, P. M., Klein, R., & Ponzetto, C. (1996). Uncoupling of Grb2 from the Met receptor in vivo reveals complex roles in muscle development. *Cell* **87**, 531-542.
- Martins, K.J.B, Gordon, T., Pette, D., Dixon, W.T., Foxcroft, G.R., Maclean, I.M. & Putman, C.T. (Submitted in 2005). Effect of satellite cell sterilization on low-frequency stimulated fast-to-slow fibre type transitions in rat skeletal muscle. *J Physiol*.
- Mauro, A. (1961). Satellite cell of skeletal muscle fibers. *J Biophys.Biochem.Cytol.* **9**, 493-495.

- McCormick, K. M. & Thomas, D. P. (1992). Exercise-induced satellite cell activation in senescent soleus muscle. *J of Applied Physiol* **72**, 888-893.
- McGeachie, J. K. (1989). Sustained cell proliferation in denervated skeletal muscle of mice. *Cell Tissue Res.* **257**, 455-457.
- McQuarrie, I. G. & Grafstein, B. (1973). Axon outgrowth enhanced by a previous nerve injury. *Arch.Neurol.* **29**, 53-55.
- McQuarrie, I. G., Grafstein, B., & Gershon, M. D. (1977). Axonal regeneration in the rat sciatic nerve: effect of a conditioning lesion and of dbcAMP. *Brain Res.* **132**, 443-453.
- McGeachie, J. K., Grounds, M. D., Partridge, T. A., & Morgan, J. E. (1993). Age-related changes in replication of myogenic cells in mdx mice: quantitative autoradiographic studies. *J Neurol.Sci.* **119** , 169-179.
- Miller, K. J., Thaloor, D., Matteson, S., & Pavlath, G. K. (2000). Hepatocyte growth factor affects satellite cell activation and differentiation in regenerating skeletal muscle. *Am J Physiol Cell Physiol* **278**, C174-C181.
- Morgan, J. E. & Partridge, T. A. (2003). Muscle satellite cells. *Int.J Biochem.Cell Biol.* **35**, 1151-1156.
- Moss, F. P. & Leblond, C. P. (1971). Satellite cells as the source of nuclei in muscles of growing rats. *Anat.Rec.* **170** , 421-435.
- Mozdziak, P. E., Schultz, E., & Cassens, R. G. (1996). The effect of in vivo and in vitro irradiation (25 Gy) on the subsequent in vitro growth of satellite cells. *Cell Tissue Res.* **283**, 203-208.
- Naumann, K. & Pette, D. (1994). Effects of chronic stimulation with different impulse patterns on the expression of myosin isoforms in rat myotube cultures. *Differentiation* **55**, 203-211.
- Oakley, B. R., Kirsch, D. R., & Morris, N. R. (1980). A simplified ultrasensitive silver stain for detecting proteins in polyacrylamide gels. *Anal.Biochem.* **105**, 361-363.



- Partridge, T. A. (2003). Stem cell route to neuromuscular therapies. *Muscle Nerve* **27**, 133-141.
- Phelan, J. N. & Gonyea, W. J. (1997). Effect of radiation on satellite cell activity and protein expression in overloaded mammalian skeletal muscle. *Anat.Rec.* **247**, 179-188.
- Putman, C. T., Dusterhoft, S., & Pette, D. (2000). Satellite cell proliferation in low frequency-stimulated fast muscle of hypothyroid rat. *Am J Physiol Cell Physiol* **279**, C682-C690.
- Putman, C. T., Dusterhoft, S., & Pette, D. (1999). Changes in satellite cell content and myosin isoforms in low-frequency-stimulated fast muscle of hypothyroid rat. *J of Applied Physiol* **86**, 40-51.
- Putman, C. T., Sultan, K. R., Wassmer, T., Bamford, J. A., Skorjanc, D., & Pette, D. (2001). Fiber-type transitions and satellite cell activation in low-frequency-stimulated muscles of young and aging rats. *J Gerontol.A Biol.Sci.Med.Sci.* **56**, B510-B519.
- Quinlan, J. G., Lyden, S. P., Cambier, D. M., Johnson, S. R., Michaels, S. E., & Denman, D. L. (1995). Radiation inhibition of mdx mouse muscle regeneration: dose and age factors. *Muscle Nerve* **18**, 201-206.
- Rabinovsky, E. D., Gelir, E., Gelir, S., Lui, H., Kattash, M., DeMayo, F. J., Shenaq, S. M., & Schwartz, R. J. (2003). Targeted expression of IGF-1 transgene to skeletal muscle accelerates muscle and motor neuron regeneration. *FASEB J* **17**, 53-55.
- Rafuse, V. F. & Gordon, T. (1996a). Self-reinnervated cat medial gastrocnemius muscles. I. comparisons of the capacity for regenerating nerves to form enlarged motor units after extensive peripheral nerve injuries. *J Neurophysiol.* **75**, 268-281.
- Rafuse, V. F. & Gordon, T. (1996b). Self-reinnervated cat medial gastrocnemius muscles. II. analysis of the mechanisms and significance of fiber type grouping in reinnervated muscles. *J Neurophysiol.* **75**, 282-297.

Rafuse, V. F., Gordon, T., & Orozco, R. (1992). Proportional enlargement of motor units after partial denervation of cat triceps surae muscles. *J Neurophysiol.* **68**, 1261-1276.

Renault, V., Piron-Hamelin, G., Forestier, C., DiDonna, S., Decary, S., Hentati, F., Saillant, G., Butler-Browne, G. S., & Mouly, V. (2000). Skeletal muscle regeneration and the mitotic clock. *Exp.Gerontol.* **35**, 711-719.

Renault, V., Thornell, L. E., Eriksson, P. O., Butler-Browne, G., Mouly, V., & Thorne, L. E. (2002). Regenerative potential of human skeletal muscle during aging. *Aging Cell* **1**, 132-139.

Roberts, P., McGeachie, J. K., & Grounds, M. D. (1997). The host environment determines strain-specific differences in the timing of skeletal muscle regeneration: cross-transplantation studies between SJL/J and BALB/c mice. *J Anat.* **191 ( Pt 4)**, 585-594.

Romanul, F. C. & Van der Meulen, J. P. (1967). Slow and fast muscles after cross innervation. Enzymatic and physiological changes. *Arch.Neurol.* **17**, 387-402.

Rosenblatt, J. D. & Parry, D. J. (1992). Gamma irradiation prevents compensatory hypertrophy of overloaded mouse extensor digitorum longus muscle. *J of Applied Physiol* **73**, 2538-2543.

Rosenblatt, J. D. & Parry, D. J. (1993). Adaptation of rat extensor digitorum longus muscle to gamma irradiation and overload. *Pflugers Arch.* **423**, 255-264.

Rosenblatt, J. D., Yong, D., & Parry, D. J. (1994). Satellite cell activity is required for hypertrophy of overloaded adult rat muscle. *Muscle Nerve* **17**, 608-613.

Sabourin, L. A. & Rudnicki, M. A. (2000). The molecular regulation of myogenesis. *Clin.Genet.* **57**, 16-25.

Schiaffino, S., Gorza, L., Pitton, G., Saggin, L., Ausoni, S., Sartore, S., & Lomo, T. (1988). Embryonic and neonatal myosin heavy chain in denervated and paralyzed rat skeletal muscle. *Dev.Biol.* **127**, 1-11.

Schiaffino, S., Gorza, L., Sartore, S., Saggin, L., Ausoni, S., Vianello, M., Gundersen, K., & Lomo, T. (1989). Three myosin heavy chain isoforms in type 2 skeletal muscle fibres. *J Muscle Res. Cell Motil.* **10**, 197-205.

Schultz E & Darr K.C. (1990). The role of satellite cells in adaptive or induced fiber transformations. Ref Type: Generic

Schultz, E. (1984). A quantitative study of satellite cells in regenerated soleus and extensor digitorum longus muscles. *Anat.Rec.* **208**, 501-506.

Schultz, E. (1989). Satellite cell behavior during skeletal muscle growth and regeneration. *Med.Sci.Sports Exerc.* **21**, S181-S186.

Schultz, E. (1996). Satellite cell proliferative compartments in growing skeletal muscles. *Dev.Biol.* **175**, 84-94.

Schultz, E. & McCormick, K. M. (1994). Skeletal muscle satellite cells. *Rev.Physiol Biochem.Pharmacol.* **123**, 213-257.

Smith, C. K., Janney, M. J., & Allen, R. E. (1994). Temporal expression of myogenic regulatory genes during activation, proliferation, and differentiation of rat skeletal muscle satellite cells. *J Cell Physiol* **159**, 379-385.

Snow, M. H. (1981). Satellite cell distribution within the soleus muscle of the adult mouse. *Anat.Rec.* **201**, 463-469.

Stonnington, H. H. & Engel, A. G. (1973). Normal and denervated muscle. A morphometric study of fine structure. *Neurology* **23**, 714-724.

Sunderland, S. & Ray, L. J. (1950). Denervation changes in mammalian striated muscle. *J Neurochem.* **13**, 159-177.

Tam, S. L., Archibald, V., Jassar, B., Tyreman, N., & Gordon, T. (2001). Increased neuromuscular activity reduces sprouting in partially denervated muscles. *J Neurosci.* **21**, 654-667.

Torrente, Y., El Fahime, E., Caron, N. J., Bresolin, N., & Tremblay, J. P. (2000). Intramuscular migration of myoblasts transplanted after muscle pretreatment with metalloproteinases. *Cell Transplant.* **9**, 539-549.

Torrente, Y., Camirand, G., Pisati, F., Belicchi, M., Rossi, B., Colombo, F., El Fahime, M., Caron, N. J., Issekutz, A. C., Constantin, G., Tremblay, J. P., & Bresolin, N. (2003). Identification of a putative pathway for the muscle homing of stem cells in a muscular dystrophy model. *J Cell Biol.* **162**, 511-520.

Totosy de Zepetnek, J. E., Zung, H. V., Erdebil, S., & Gordon, T. (1992a). Innervation ratio is an important determinant of force in normal and reinnervated rat tibialis anterior muscles. *J Neurophysiol.* **67**, 1385-1403.

Totosy de Zepetnek, J. E., Zung, H. V., Erdebil, S., & Gordon, T. (1992b). Motor-unit categorization based on contractile and histochemical properties: a glycogen depletion analysis of normal and reinnervated rat tibialis anterior muscle. *J Neurophysiol.* **67**, 1404-1415.

Viguie, C. A., Lu, D. X., Huang, S. K., Rengen, H., & Carlson, B. M. (1997). Quantitative study of the effects of long-term denervation on the extensor digitorum longus muscle of the rat. *Anat.Rec.* **248**, 346-354.

Wheldon, T. E., Michalowski, A. S., & Kirk, J. (1982). The effect of irradiation on function in self-renewing normal tissues with differing proliferative organisation. *Br.J Radiol.* **55**, 759-766.

Wright, W. E., Piatyszek, M. A., Rainey, W. E., Byrd, W., & Shay, J. W. (1996). Telomerase activity in human germline and embryonic tissues and cells. *Dev.Genet.* **18**, 173-179.

Wakeford, S., Watt, D. J., & Partridge, T. A. (1991). X-irradiation improves mdx mouse muscle as a model of myofiber loss in DMD. *Muscle Nerve* **14**, 42-50.

Yablonka-Reuveni, Z. & Rivera, A. J. (1994). Temporal expression of regulatory and structural muscle proteins during myogenesis of satellite cells on isolated adult rat fibers. *Dev.Biol.* **164**, 588-603.

Yoshida, N., Yoshida, S., Koishi, K., Masuda, K., & Nabeshima, Y. (1998). Cell heterogeneity upon myogenic differentiation: down-regulation of MyoD and Myf-5 generates 'reserve cells'. *J Cell Sci.* **111 ( Pt 6)**, 769-779.

Zhang, M. & McLennan, I. S. (1994). Use of antibodies to identify satellite cells with a light microscope. *Muscle Nerve* **17**, 987-994.